Kinetics of Bicarbonate and Chloride Transport in Human Red Cell Membranes

PEDER K. GASBJERG and JESPER BRAHM

From the Department of General Physiology and Biophysics, The Panum Institute, University of Copenhagen, DK-2200 Copenhagen N, Denmark

ABSTRACT Unidirectional [^{14}C]HCO_3^- and $^{36}Cl^-$ efflux from human red cells and ghosts was studied under self-exchange conditions at pH 7.8 and 0°C by means of the Millipore-Swinnex filtering technique. Control bicarbonate experiments showed that $^{14}CO_2$ loss from the cells to the efflux medium was insignificant. The anion flux was determined under (*a*) symmetric variations of the anion concentration ($C^{(i)} = C^{(o)}$ = 5–700 mM), and (*b*) asymmetric conditions with C_{An} constant on one side and varied on the other side of the membrane. Simple Michaelis-Menten–like kinetics (MM fit: $J^{eff} = J^{eff}_{max} \cdot C/(K_{1/2} + C)$) was used to describe anion flux dependence on C for (*a*) $C^{(i)} = C^{(o)}$ = 5–100 mM, (*b*) $C^{(i)}$ = 6–100 mM, $C^{(o)}$ = constant, and (*c*) $C^{(i)}$ = constant, $C^{(o)}$ = 1–25 mM. At higher cellular concentrations noncompetitive self-inhibition by anion binding (inhibition constant K_i mM) to an intracellular site was included in the model (MS fit): $J^{eff} = J^{eff}_{max} \cdot C^{(i)}/[(K_{1/2} + C^{(i)}) \cdot (1 + C^{(i)}/K_i)]$. The MM fits show that the external half-saturation constant, $K^o_{1/2}$ (= $C^{(o)}_{An}$ for $J^{eff,o} = 1/2 \cdot J^{eff,o}_{max}$) at $C^{(o)}$ = 1–25 mM is 1.5–2.4 mM (HCO_3^-) and 1.8–2.6 mM (Cl^-). At $C^{(o)}$ = 1–260 mM $K^o_{1/2}$ is 1.2–1.5 mM (HCO_3^-) and 1.4–1.8 mM (Cl^-). The respective maximum flux, $J^{eff,o}_{max}$ (nmol/[cm^2·s]), for $C^{(o)}$ = 1–25 mM is 0.41–0.51 (HCO_3^-) and 0.28–0.38 (Cl^-), and for $C^{(o)}$ = 1–260 mM 0.39–0.44 (HCO_3^-) and 0.27–0.31 (Cl^-). The internal half-saturation constant, $K^i_{1/2}$ mM is: MM fit ($C^{(i)}$ = 6–100 mM, $C^{(o)}$ = 50 mM), 18.0 mM (HCO_3^-) and 23.8 mM (Cl^-); MS fit ($C^{(i)}$ = 6–920 mM, $C^{(o)}$ = 50 mM), 32.0 mM (HCO_3^-) and 45.1 mM (Cl^-). The maximum flux, $J^{eff,i}_{max}$ (nmol/[cm^2·s]) is: MM fit; 0.50 (HCO_3^-) and 0.34 (Cl^-); MS fit, 0.70 (HCO_3^-) and 0.50 (Cl^-). The half-inhibition constants of the MS fit, K_i, are 393 mM (HCO_3^-) and 544 mM (Cl^-). The MM fit shows that the symmetric half-saturation constant, $K^s_{1/2}$, is 20.2 (HCO_3^-) and 23.9 (Cl^-) mM, and $J^{eff,s}_{max}$ is 0.51 (HCO_3^-) and 0.32 (Cl^-) nmol/(cm^2·s). The MS fit shows that for C = 5–700 mM $K^s_{1/2}$ is 30.4 mM (HCO_3^-) and 50.1 mM (Cl^-), and K_i is 541 mM (HCO_3^-) and 392 mM (Cl^-). In both fits the K_i values for HCO_3^- and Cl^- are not significantly different. The functional asymmetry of the transport system was demonstrated for both anions, independent of any model, in two reversed experiments with either internal or external 50 mM anion and a varied concentration on the opposite side. The apparent affinity for both anions is ~10 times higher on the

Address reprint requests to Dr. Jesper Brahm, Department of General Physiology and Biophysics, The Panum Institute, University of Copenhagen, Blegdamsvej 3, DK-2200 Copenhagen N, Denmark.

J. GEN. PHYSIOL. © The Rockefeller University Press · 0022-1295/91/02/0321/29 $2.00 321
Volume 97 February 1991 321–349

outside than on the inside (MM fit). According to the "ping-pong" model, $K^{o}_{1/2}$ and $K^{s}_{1/2}$ can be used to calculate an asymmetry factor (A). In our study A is 0.12 ± 0.02 for both anions if the results obtained in the low concentration ranges are used; i.e., eight times more unloaded transport sites face inward than outward when $C^{(i)} = C^{(o)}$. If the results of the whole concentration range are used, A_{Cl} is 0.05 ± 0.01 and A_{bic} is 0.06 ± 0.01. Hence, A does not depend on which anion is transported, but the magnitude of A depends on which concentration range and fitting procedure are used to determine the factors that can be used to calculate A.

INTRODUCTION

Capnophorin, the anion exchange protein of the erythrocyte membrane, is asymmetric in both position and function (see, for example, Macara and Cantley, 1983; Brahm, 1986; Knauf, 1986; Passow, 1986).

Previous studies of chloride transport in human red cells have demonstrated a functional asymmetry at 0°C that appears more pronounced at physiological temperatures (Gunn and Fröhlich, 1979; Schnell, 1979; Furuya et al., 1984, Knauf et al., 1984; Knauf and Brahm, 1989). The proposed "ping-pong" model for anion exchange in the red cell membrane suggests that a transport site, unloaded or loaded with an anion, may be either internally or externally located, and that translocation of the unloaded forms is negligible as compared with the translocation of the loaded forms. The functional asymmetry of the transporter can be expressed by an asymmetry factor, A, which expresses the ratio of unloaded transport sites facing outward and inward under conditions where the anion concentrations on the two sides of the membrane are equal. The model predicts simple saturation kinetics for unidirectional anion efflux under symmetric variations of the anion concentration $C^{(i)} = C^{(o)}$, and under asymmetric conditions with a constant anion concentration on one side of the membrane and a varied anion concentration on the other side of the membrane. The functional asymmetry appears as different apparent affinities for the monovalent anion on the inside ($K^{i}_{1/2}$) and outside ($K^{o}_{1/2}$) of the membrane. A can be calculated as the ratio of $K^{o}_{1/2}$ to $K^{i}_{1/2}$ if the fixed *trans*-concentrations are saturating. A can also be calculated by using the half-saturation constant for a symmetric variation ($K^{s}_{1/2}$) and $K^{o}_{1/2}$ (see Appendix). The kinetics of the model further predicts that A is independent of which monovalent inorganic anion is transported (Fröhlich and Gunn, 1986; Knauf, 1986). For chloride transport at 0°C A has been determined to be 1/15 = 0.064 (Brazy and Gunn, 1976; Gunn and Fröhlich, 1979); that is, 15 times more unloaded sites face inward than outward when $Cl^{-(o)} = Cl^{-(i)}$. More recent results suggest a less marked asymmetry (Hautmann and Schnell, 1985).

Kinetics of anion transport at both 0 and 38°C (Dalmark, 1976; Brahm, 1977; Wieth and Brahm, 1980) show, however, that the simple Michaelis-Menten–like kinetics do not describe the anion transport at higher concentrations, where anion transport decreases ("self-inhibition;" Dalmark, 1976). Self-inhibition has been interpreted in terms of a modifier site in the vicinity of the transport site that modulates transport upon binding of an anion (Dalmark, 1976). The degree of self-inhibition depends on which anion is transported and on the temperature. Dalmark's study at 0°C suggests that bicarbonate ions are less self-inhibitory than the other inorganic monovalent anions, whereas bicarbonate shows a much more pronounced self-

inhibition at body temperature than chloride (Brahm, 1977; Wieth and Brahm, 1980). From a kinetic point of view bicarbonate should be the anion of choice for asymmetry studies of the anion transport system at 0°C if self-inhibition is neglected. However, the functional asymmetry has been determined by means of chloride, which is less demanding in the experimental procedures.

We performed parallel experiments with bicarbonate and chloride to determine the asymmetry factor for both anions under similar experimental conditions. Our study shows that self-inhibition effects the calculated asymmetry factor even in the physiological concentration range. Although the simple Michaelis-Menten equation fits well to the experimental data in the range 6–100 mM in experiments where $C^{(i)}$ is varied and $C^{(o)}$ is constant or varied, the calculated unidirectional fluxes in this range might be significantly reduced by intracellular, noncompetitive self-inhibition. An extension of the concentration range up to 900 mM reveals that the simple Michaelis-Menten equation cannot be used at higher concentrations, because the measured flux values at high concentrations are lower than predicted from the values obtained at lower concentrations. If we assume that the deviation of the data from the simple Michaelis-Menten equation is caused by intracellular, noncompetitive self-inhibition, the phenomenon can be included in the ping-pong model as binding of an anion to one intracellular site. If the modified model is applied on the experimental results in the concentration range 6–900 mM, the estimated values for $K^s_{1/2}$ and $K^i_{1/2}$ for both anions increase by 1.5–2 times the values obtained in the range 6–100 mM by means of the simple ping-pong model, and the calculated asymmetry factors are significantly reduced. Both methods were applied to each experimental series involving intracellular concentration changes yielding two sets of estimated values of $K^s_{1/2}$ and $K^i_{1/2}$ for both anions.

We also found that although self-inhibition is predominantly intracellular, a deviation from the simple Michaelis-Menten kinetics appears even in the experimental series with $C^{(i)}$ = constant and $C^{(o)}$ varied. The unidirectional efflux of both anions shows a small maximum of the efflux curve at $C^{(o)} \approx$ 15–30 mM. The calculated outside half-saturation constant, $K^o_{1/2}$, is dependent on which extracellular concentration range is used for data analysis. As the somewhat scattered data do not allow a quantitative incorporation of this local maximum phenomenon in the ping-pong model as a partial extracellular self-inhibition, we illustrate it by fitting the simple Michaelis-Menten equation to the experimental data twice: first in a limited concentration range (1–25 mM), and second in the complete experimental concentration range yielding two values of $K^o_{1/2}$ for each experimental series.

As the fitting procedures yield two half-saturation constants for each experimental series, we can calculate four values of A for each anion using different combinations of the estimated values of $K^s_{1/2}$ and $K^o_{1/2}$. Our results suggest that the asymmetry factor for bicarbonate and chloride transport is in the range 0.05–0.12.

MATERIALS, METHODS, AND CALCULATIONS

Media

All media were prepared from grade chemicals and had the following compositions (in mM): Medium A: 1–880 KCl, 0.5 KH_2PO_4. Medium B: 1–920 $KHCO_3$, 1 acetazolamide. In both

media sucrose was used as the osmotic active substituent. Medium C: 5–700 $KHCO_3$, 1 acetazolamide, or 5–700 KCl, 0.5 KH_2PO_4. At concentrations <100 mM anion sucrose was added to keep osmolarity equal to that of the resealed ghosts. Medium D: 4 $MgSO_4$, 3.8 acetic acid. Medium E: 0–3,000 KCl, 0–1,000 sucrose to replace KCl, 25 Tris, 12 acetazolamide (Sigma Chemical Co., St. Louis, MO). Medium F: 165 $KHCO_3$, 0.05 4,4′-diisothiocyanostilbene-2,2′-disulfonic acid (DIDS). DIDS was used from a 10-mM stock solution that was stored frozen. Media A, B, C, and F were titrated to pH 7.8 at 0°C with 1 N H_3PO_4 (bicarbonate), HCl (chloride), or KOH, and were used for efflux experiments. Medium G: 0–165 KCl, 0–165 $KHCO_3$, 0–1 acetazolamide, 0–0.5 KH_2PO_4. The chloride and bicarbonate concentrations were varied by mixing media A-165 and B-165, that is C_{anion} = 165 mM. H_3PO_4 or KOH was used for titration. Osmolarity of the media was measured using a Roebling Micro Osmometer (Messtechnik, Berlin, Germany).

Curve Fitting

All fittings of mathematical functions (except straight lines) to experimental data were performed using nonlinear, least-squares regression analysis (StatGraphics; STSC, Inc., Rockville, MD). The program calculates a standard error (SE) of the estimated parameters.

Physical Chemistry of the Bicarbonate Solutions

In aqueous solutions CO_2 equilibrates according to

$$CO_2 + H_2O \rightleftarrows H_2CO_3 \rightleftarrows HCO_3^- + H^+ \rightleftarrows 2H^+ + CO_3^=$$

The relative amount of each substance depends on pH. At pH 7.8 the relative amount of H_2CO_3 is very small and negligible. At equilibrium the ratio between the concentrations of bicarbonate and CO_2 follows from the Henderson-Hasselbalch equation: $pH = pK_a + \log(HCO_3^-/CO_2)$. We used the data of Harned and Bonner (1945) to obtain a pK_a of ~6.30 at 160 mM (0°C). As the glass electrode (a calomel electrode as reference) measured the H^+ activity, we adjusted the value of pK_a by using an extended Debye-Hückel expression to calculate the activity coefficient for H^+ at an ionic strength of 160 mM. The adjusted pK_a value was 6.39 and the experimental pH was 7.8; hence, the Henderson-Hasselbalch equation yields HCO_3^-/CO_2 = 25.7. We calculated the ratio $HCO_3^-/CO_3^=$ to be 302, based on the results of Harned and Scholes (1941). Hence, the composition of a 165-mM bicarbonate solution at pH 7.8 and 0°C is 6.2 mM CO_2, 158.3 mM HCO_3^-, and 0.5 mM $CO_3^=$. As the ionic strength of the solution is lowered, the fraction of CO_2 is slightly increased. Our calculations show that the "true" (actual) bicarbonate concentration is >94% of the "nominal" bicarbonate concentration in all experiments, and we therefore used the nominal bicarbonate concentrations in the flux calculations.

The presence of $^{14}CO_2$ in bicarbonate solutions offers three major problems in bicarbonate efflux experiments. First, when packed cells loaded with $[^{14}C]HCO_3^-$ are suspended in the efflux medium in the flux chamber, intracellular $^{14}CO_2$ rapidly equilibrates across the membrane and contributes to the background radioactivity. Second, the continuous intracellular conversion of $[^{14}C]HCO_3^-$ to $^{14}CO_2$ (during the efflux experiment), which is followed by a rapid efflux of $^{14}CO_2$, may be significant compared with the efflux of $[^{14}C]HCO_3^-$. Third, $^{14}CO_2$ may be lost from the cell suspension during the efflux experiment. All three factors may affect the determination of the efflux rate constant for $[^{14}C]HCO_3^-$.

Preparation of Red Cells and Ghosts

Freshly drawn, heparinized blood samples from either of the two healthy authors were used in all experiments on the same day, except for the anion substitution experiment where the resealed ghosts were stored cold for ~24 h. Red cells were washed one time in medium A-150

or medium B-150 (pH 7.8), titrated to be in equilibrium with external pH ($pH^{(i)}$ ~7.65 according to the anion distribution ratio [cf. Eq. 4 in Funder and Wieth, 1966]), and subsequently washed three more times in the appropriate medium. Cells washed in medium B were incubated at 38°C for 20 min between each wash to equilibrate acetazolamide. Next, the cells were loaded with the radioactive isotope and packed as described below. Resealed ghosts were made in a modified version of that described by Schwoch and Passow (1973) (Schnell, K., personal communication): After one wash in 165 mM KCl the cells were resuspended to the original volume, lysed by adding 10 times the volume of medium D (0°C, pH 5.9–6.2, pH adjusted with 2 M Tris), and incubated for 5 min before addition of medium E. "Ordinary" ghosts were made by adding a volume equal to the original volume (1/11 of the total volume) of 2 M KCl, 25 mM Tris, and 12 mM acetazolamide. By dilution the ghosts contained ~165 mM KCl, 2 mM Tris, and 1 mM acetazolamide. Resealing of the ghosts was completed by incubation at 38°C, pH 7.8, for 45 min. Ghosts with higher or lower chloride concentrations were made by varying either the relative volume of medium E, the composition of medium E with respect to the KCl concentration, or both factors. If the volume of medium E was changed, the concentrations of acetazolamide and Tris were adjusted to keep final cellular concentrations of 1 and 2 mM, respectively (low chloride ghosts [5 mM] were made by adding 20 times the volume of medium D). At final KCl concentrations <100 mM sucrose was added to medium E to obtain an average volume of the different ghost samples of 60–110 fl. After resealing was completed, the cells were washed several times in either medium A or C. By washes in medium C cell chloride was completely exchanged for bicarbonate as indicated by the distribution of radioactively labeled bicarbonate (see below). In anion substitution experiments resealed chloride ghosts were washed three times in medium G to make intra- and extracellular bicarbonate and chloride concentrations equal.

In control experiments bicarbonate transport was maximally inhibited by means of DIDS. Red cells at a cytocrit of 50% were incubated in medium F for 30 min at 38°C, which ensured maximal inhibition of anion transport (Janas et al., 1989). Subsequently, resealed ghosts were made as described above, with the exception that KCl was replaced by $KHCO_3$ in medium E. The ghosts were incubated with $[^{14}C]HCO_3^-$ for 20 min at 38°C. The efflux medium also contained 50 μM DIDS.

Determination of Radioactivity, Intracellular Anion Concentration, and Cell Water Volume

The red cells or ghosts were loaded with ^{36}Cl (AEK, Risø, Denmark), $[^{14}C]HCO_3^-$ (Amersham Corp., Buckinghamshire, UK), or both isotopes (substitution experiments), 0.5 μCi (18 kBq) per ml cell suspension with a cytocrit of ~50%. The cells were packed in nylon tubes (see Funder and Wieth, 1967) by centrifugation at 50,000 *g* for 15 min, and separated from the supernate by cutting the tubes. The radioactivity in the cell sample and supernate, as well as the cell-free filtrates from the efflux experiments (see below), were determined by β-liquid scintillation spectrometry of the samples suspended in Optifluor (Tricarb; Packard Instrument Co., Inc., Downers Grove, IL). Since the hemoglobin content in the ghosts was <2% (wt/vol), the radioactivity of the equilibrium samples of experiments with $C^{(i)} \approx C^{(o)}$ was counted directly. In anion substitution experiments the $[^{14}C]HCO_3^-$ activity was corrected for interference from ^{36}Cl using an internal standard, and ^{36}Cl activity was measured above the maximum β-energy for $[^{14}C]$ and was not corrected. In ghost experiments with low extracellular anion concentrations, and in all experiments with red cells, a cell-free sample was obtained for counting after isotopic equilibrium was reached (more than seven half-times).

For bicarbonate it was assumed that the distribution ratios between the cells and the wash medium of $[^{14}C]$ and HCO_3^- were identical ($R = [^{14}C]^{(i)}/[^{14}C]^{(o)} = HCO_3^{-(i)}/HCO_3^{-(o)}$). The contribution to *R* from dissolved $^{14}CO_2$ (whose distribution ratio was equal to 1) was negligible at pH 7.8. The fraction of physically dissolved CO_2 at pH 7.8 was 3–6%, depending on the ionic

strength of the medium. Binding of $^{14}CO_2$ to amino groups in the cells had a minor influence on R in red cells. In resealed ghosts with hemoglobin concentration <3% of the content in control cells, the contribution of carbamino-bound $^{14}CO_2$ to R could be neglected. For bicarbonate, R was determined by a dilution analysis. The packed cells of a nylon tube (X g) were mixed with P ml of the wash medium (C) and a few minutes later a filtered sample was taken for scintillation counting. R was calculated from the equation

$$R = [C_a \cdot (Z + P/X) - Z \cdot B_b]/[(B_b - C_a) \cdot (F_m - Z)] \quad (1)$$

where Z is milliliters of trapped extracellular medium per gram packed cells, X is grams of packed cells, F_m is milliliters water per gram packed cells, and C_a and B_b are the concentrations of [^{14}C] activity in the filtered sample and the supernate of the nylon tube, respectively. For chloride, R was determined by cell precipitation with perchloric acid (Dalmark and Wieth, 1972). The intracellular bicarbonate or chloride concentration, $C^{(i)}$, was calculated from $C^{(i)} = C^{(o)} \cdot R$.

Red cell water content (volume) was determined in each experiment by drying a cell sample to constant weight. In experiments with ghosts we assumed that cell water was 97% of the cell volume (Brahm, 1977, 1982), which was determined by Coulter counting (model DN; Coulter Electronics, Inc., Hialeah, FL). The determinations were corrected for extracellular trapped volume in the cell samples. [^{14}C]Inulin that does not permeate the cell membrane was used to determine the trapped volume. Usually, a trapped volume of 2% in samples of packed RBC and 8% in packed red cell ghost was used.

Determination of the Rate of Efflux

All experiments were carried out at pH 7.8 and 0°C under conditions of self-exchange to measure the tracer ($^{36}Cl^-$ or [^{14}C]HCO_3^-) efflux rate (k', s^{-1}) as described elsewhere (Funder and Wieth, 1976; Wieth, 1979).

In experiments where the intra- and extracellular amounts of solute (bicarbonate or chloride) were comparable in magnitude, k' was corrected to obtain the "true" unidirectional efflux rate coefficient, k:

$$k = k' \cdot V^{(o)}/(V^{(o)} + r \cdot V^{(i)}) \quad (2)$$

where r is the ratio between the concentrations of intra- and extracellular bicarbonate or chloride ($r = R$ if the efflux medium is identical to the wash medium), $V^{(i)}$ is the total cell water volume, and $V^{(o)}$ is the volume of the efflux medium.

Calculation of Flux

The unidirectional chloride or bicarbonate efflux is defined as

$$J^{eff} = k \cdot (V_c^{(i)}/A_c) \cdot C^{(i)} \text{ (mol/[cm}^2 \cdot \text{s])} \quad (3)$$

where k is the ^{36}Cl or [^{14}C]HCO_3^- efflux rate coefficient (s^{-1}), $V_c^{(i)}$ is the cell water volume (cm^3), $C^{(i)}$ is the intracellular anion concentration (mol/cm^3), and A_c is the cell surface area that is assumed to be constant $1.42 \cdot 10^{-6}$ cm^2/cell (see Brahm, 1982).

RESULTS

Control Experiments

Control experiments were performed to evaluate the applicability of the method to determine [^{14}C]HCO_3^- efflux. The semilogarithmic plot of Fig. 1 *A* shows the results

of [^{14}C]HCO_3^- efflux (filled circles) and ^{36}Cl efflux (open circles) from intact red cells under conditions of self-exchange at pH 7.8 (0°C). The ordinate expresses the fraction of tracer that remains intracellular at the time of sampling. The linearity of the plots indicates that first-order kinetics apply to both transport processes. Because of the experimental conditions of a low hematocrit (< 1%) the numerical value of the slope of the plot (k, s^{-1}) equals the rate coefficient of the transport process. In Fig. 1 *A* k_{bic} = 0.074 and k_{Cl} = 0.050 s^{-1}, indicating that bicarbonate is transported ~50% faster than chloride under similar experimental conditions.

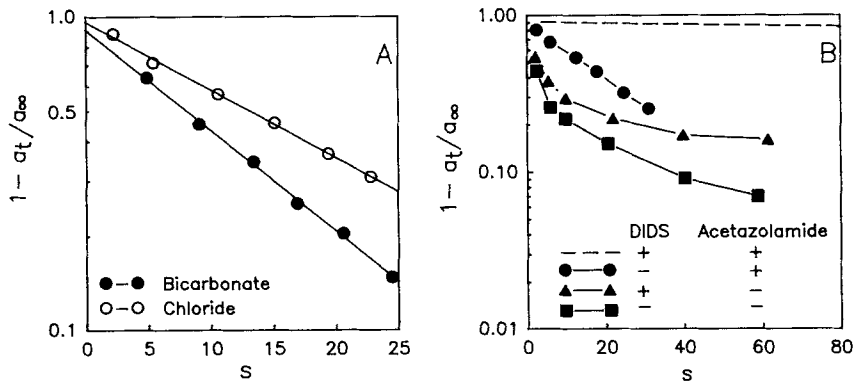

FIGURE 1. Efflux rate of [^{14}C]HCO_3^- (*filled symbols*) and $^{36}Cl^-$ (*open symbols*) from human red cells under conditions of self-exchange (*A*) and [^{14}C] from resealed red cell ghosts (*B*) at 0°C and pH 7.8. The logarithmic ordinates depict the intracellular fraction of radioactive isotope in the cells at time t. The interception of the plots with the ordinate represents (*a*) radioactivity trapped between the cells during the packing procedure and (*b*) any intracellular radioactivity that had equilibrated rapidly across the membrane before the sampling procedure was started. The numeric value of the slope of the plots equals the rate coefficients of the transport processes. (*A*) The anion concentrations were similar in the two experiments with intact red cells: $C^{(i)}$ = 100 mM and $C^{(o)}$ = 150 mM. The carbonic anhydrase was maximally inhibited by 1 mM acetazolamide. The half-time ($T_{1/2}$) was 13.9 s (k = 0.050 s^{-1}) for chloride and 9.4 s (k = 0.074 s^{-1}) for bicarbonate self-exchange. (*B*) Four experiments of [^{14}C] efflux from radioactive, loaded, resealed red cell ghosts. The bicarbonate efflux rate of control cells was 0.040 s^{-1}. Treatment with the anion transport inhibitor DIDS inhibited bicarbonate efflux by > 98%. In absence of acetazolamide, a larger fraction of the intracellular radioactivity in the form of $^{14}CO_2$ was rapidly released from the cells as indicated by the curvature of the plots (for further details, see Discussion).

Fig. 1 *B* shows four plots of [^{14}C]HCO_3^- efflux from resealed red cell ghosts whose carbonic anhydrase content was greatly reduced (> 97%) by the procedure of making the ghosts. The control cells (circles) exchange bicarbonate with a rate of 0.040 s^{-1} ($T_{1/2}$ = ln 2/k = 17 s). The residual carbonic anhydrase activity was inhibited by means of 1 mM acetazolamide that was used to inhibit the enzyme activity maximally in intact red cells. Exposure of the ghost cells to 50 μM 4,4′-diisothiocyano-2,2′-stilbenedisulfonate (DIDS) that maximally inhibits chloride transport in ghosts

(~99.7%) inhibited the efflux of [^{14}C] radioactivity by 98.3% (dashed line). The flux medium also contained 50 μM DIDS.

The two other plots of Fig. 1 *B* (triangles and squares) are results obtained with ghosts that were not incubated with acetazolamide. Although the carbon anhydrase concentration in ghosts was reduced during the preparation procedure to <3% of the concentration in control ghosts, the activity was still high enough to cause a significant loss of radioactivity within the first 10 s, as indicated by the first steep part

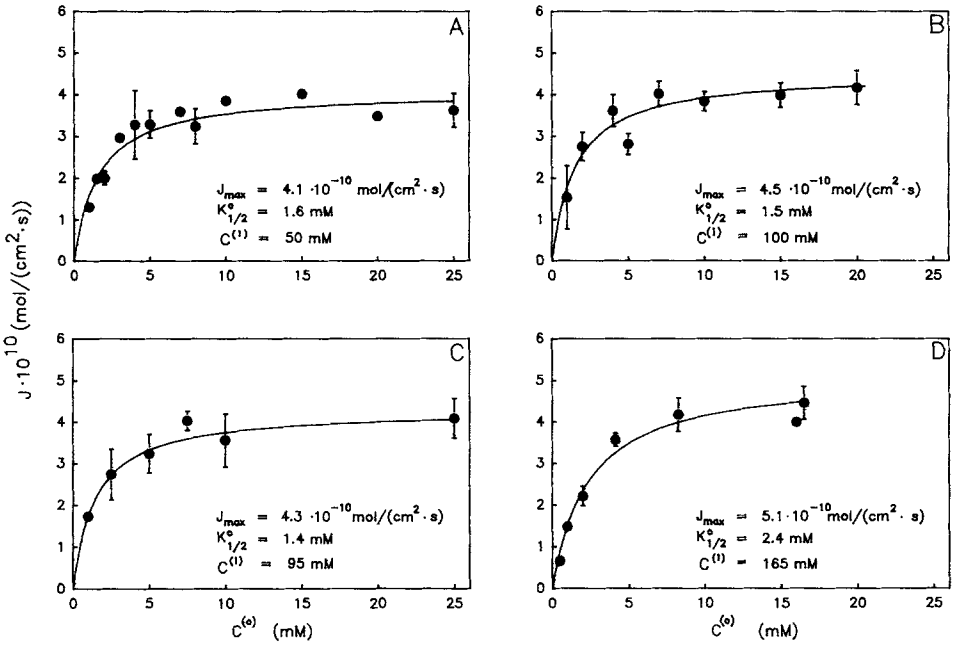

FIGURE 2. Plots of bicarbonate efflux (0°C, pH 7.8) under conditions of constant intracellular concentration and varied extracellular concentration. *A*, *B*, and *D* show bicarbonate efflux from resealed red cell ghosts with $C^{(i)}$ = 50, 100, and 165 mM, respectively. *C* depicts bicarbonate efflux from intact red cells with $C^{(i)}$ = 95 mM. Sucrose replaced external bicarbonate, and was added to the internal solution when $C^{(i)}_{bic}$ = 50 mM and $C^{(o)}_{bic}$ > 165 mM. Each point represents an average of two or more experiments. The standard deviation of the flux values, as indicated by bars if they exceed the point, represent the standard deviation of the rate coefficient used to calculate the flux (cf. Methods). In all four plots the curve was fitted to a simple Michaelis-Menten–like expression within the concentration range of $C^{(o)}$ = 1–25 mM, which was the arbitrarily set upper limit. Values of J_{max} and $K_{1/2}$ were obtained by a nonlinear fitting program.

of the plots. The rate of efflux of radioactivity gradually became slower both in ghosts not exposed to DIDS (squares) and in ghosts exposed to DIDS (triangles) (see Discussion).

The Kinetics of Chloride and Bicarbonate Transport

The kinetics of chloride and bicarbonate transport were studied under three different conditions: (*a*) cell anion concentration is constant, extracellular anion concentration

varies; (*b*) extracellular anion concentration is constant, cell anion concentration varies; and (*c*) intra- and extracellular anion concentration vary simultaneously.

(a) Cell anion concentration is constant; extracellular anion concentration varies. As only the external anion concentration is varied (with sucrose simply replacing KCl or $KHCO_3$), the experiments can be done with both intact red cells and resealed red cell ghosts. Figs. 2 and 3 show bicarbonate results, and Figs. 4 and 5 show the results of chloride obtained with intact red cells and resealed ghosts. We determined the half-saturation constant and maximum flux under asymmetric conditions in red cells and resealed ghosts with intracellular bicarbonate concentrations of 50, 95 (RBC), 100, and 165 mM, and chloride concentrations of 50, 100, 107 (RBC), and 165 mM

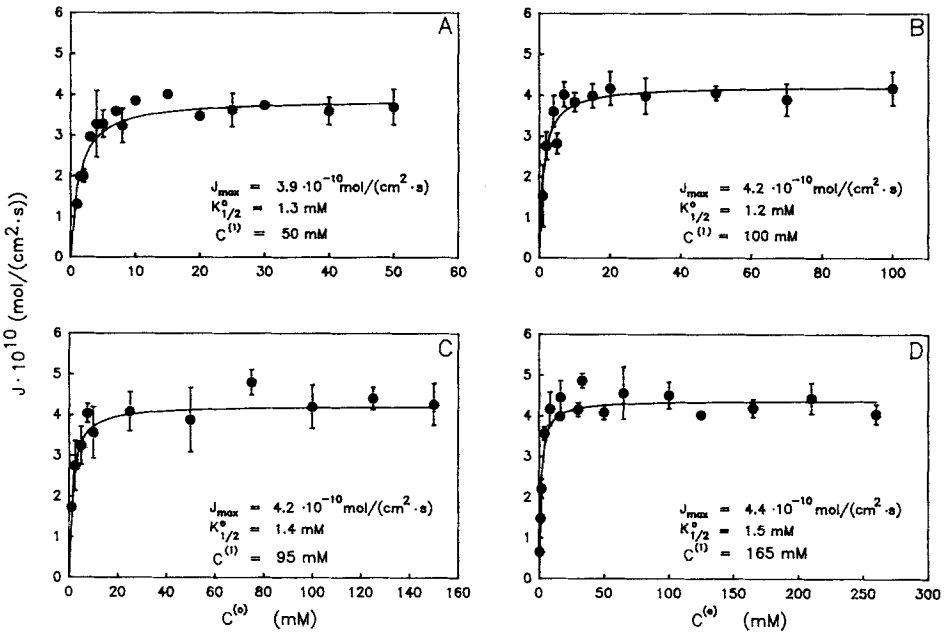

FIGURE 3. Bicarbonate efflux (0°C, pH 7.8) from resealed red cell ghosts (*A*, $C^{(i)}$ = 50 mM; *B*, $C^{(i)}$ = 100 mM; *D*, $C^{(i)}$ = 165 mM) and intact red cells (*C*, $C^{(i)}$ = 95 mM) suspended in media with $C^{(o)}$ from 1 to 260 mM. Sucrose replaced bicarbonate to balance internal and external osmolarities.

by varying the extracellular concentration ranging from 1 mM up to the intracellular concentration. In the eight experimental series with fixed internal chloride or bicarbonate concentrations in the range 50–165 mM the self-exchange flux (ordinates) saturates by an increase of the extracellular anion concentration to ~20 mM. In the experiments with ghosts having $C^{(i)}$ = 165 mM, $C^{(o)}$ was increased further to ~250 mM. When $C^{(o)} > C^{(i)}$ sucrose was added to the resealing medium to keep internal and external osmolarities equal. The addition of sucrose to the resealing medium reduced cell volume and increased the efflux rate constant. However, control experiments (data not shown) show that the unidirectional flux was not

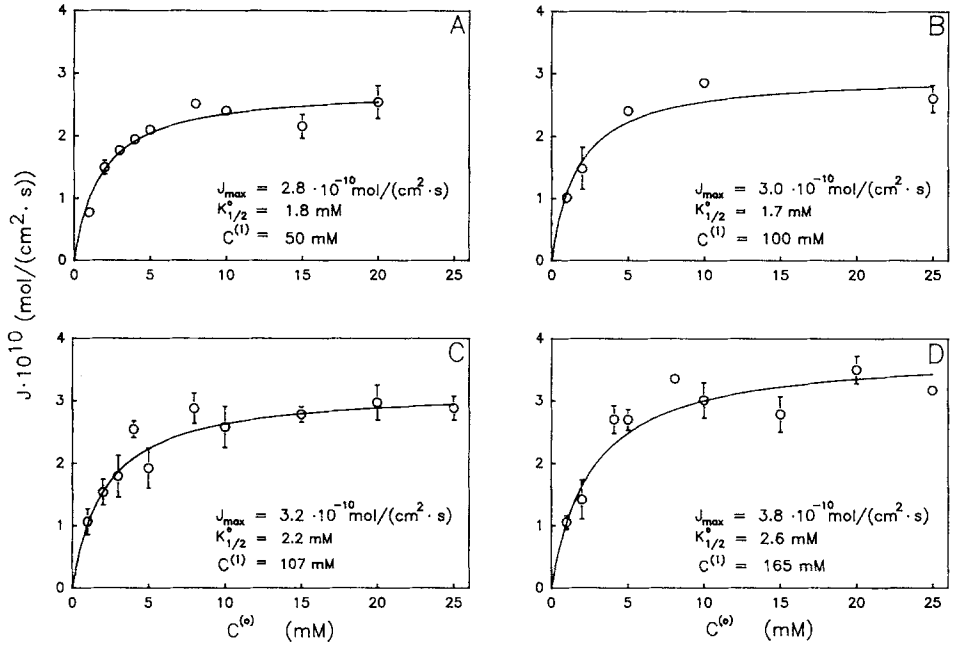

FIGURE 4. Same conditions as described in the legend to Fig. 2, with the exceptions that bicarbonate was replaced by chloride, and $C^{(i)}$ in the intact red cells was 107 mM.

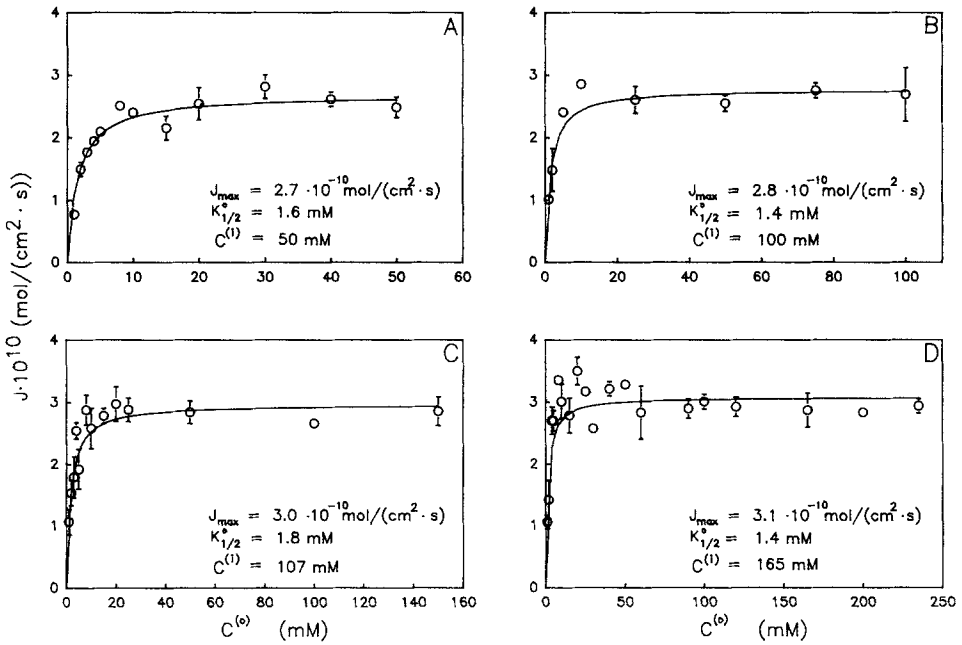

FIGURE 5. Same conditions as described in the legend to Fig. 3, with the exceptions that bicarbonate was replaced by chloride, and $C^{(i)}$ in the intact red cells was 107 mM.

TABLE I

Kinetic Parameters for Bicarbonate and Chloride Self-Exchange in Human Red Blood Cells and Ghosts at 0°C, pH 7.8

Type of experiment	Concentration		Fit	$J_{max} \cdot 10^{10}$	$K_{1/2}$	K_i	A^*	$1/A^*$
	Fixed	Range						
Bicarbonate	*mM*			*mol/(cm²·s)*		*mM*		
G,OV	50	1–25	MM	4.1 ± 0.2	1.6 ± 0.3	—	0.118	8.5
G,OV	100	1–25	MM	4.5 ± 0.2	1.5 ± 0.3	—	0.099	10.2
R,OV	95	1–25	MM	4.3 ± 0.2	1.4 ± 0.4	—	0.093	10.7
G,OV	165	1–25	MM	5.1 ± 0.2	2.4 ± 0.3	—	0.149	6.7
G,IV	50	1–100	MM	5.0 ± 0.2	18.0 ± 2.4	—	—	—
G,S	—	1–100	MM	5.1 ± 0.2	20.2 ± 1.9	—	—	—
						Mean:	0.115	8.7
						SD:	0.025	1.8
G,OV	50	1–50	MM	3.9 ± 0.1	1.3 ± 0.2	—	0.071	14.0
G,OV	100	1–100	MM	4.2 ± 0.1	1.2 ± 0.2	—	0.055	18.0
R,OV	95	1–150	MM	4.2 ± 0.1	1.4 ± 0.3	—	0.064	15.7
G,OV	165	1–260	MM	4.4 ± 0.1	1.5 ± 0.2	—	0.060	16.6
G,IV	50	6–920	MS	7.0 ± 0.6	32.0 ± 5.5	393 ± 68	—	—
G,S	—	5–700	MS	6.6 ± 0.3	30.4 ± 3.0	541 ± 71	—	—
						Mean:	0.062	16.0
						SD:	0.007	1.7
Chloride								
G,OV	50	1–25	MM	2.8 ± 0.1	1.8 ± 0.3	—	0.119	8.4
G,OV	100	1–25	MM	3.0 ± 0.1	1.7 ± 0.3	—	0.097	10.3
R,OV	107	1–25	MM	3.2 ± 0.1	2.2 ± 0.3	—	0.122	8.2
G,OV	165	1–25	MM	3.8 ± 0.1	2.6 ± 0.4	—	0.142	7.0
G,IV	50	6–100	MM	3.4 ± 0.2	23.8 ± 3.1	—	—	—
G,S	—	5–100	MM	3.2 ± 0.2	23.9 ± 3.4	—	—	—
						Mean:	0.120	8.3
						SD:	0.018	1.4
G,OV	50	1–50	MM	2.7 ± 0.1	1.6 ± 0.2	—	0.065	15.3
G,OV	100	1–100	MM	2.8 ± 0.1	1.4 ± 0.3	—	0.044	22.8
R,OV	107	1–150	MM	3.0 ± 0.1	1.8 ± 0.2	—	0.053	18.7
G,OV	165	1–235	MM	3.1 ± 0.1	1.4 ± 0.2	—	0.038	26.5
G,IV	50	6–880	MS	5.0 ± 0.5	45.1 ± 7.6	544 ± 102	—	—
G,S	—	5–700	MS	5.1 ± 0.6	50.1 ± 9.5	392 ± 94	—	—
						Mean:	0.050	20.0
						SD:	0.012	4.9

G, resealed ghosts; R, intact red blood cells; OV, asymmetric anion distribution ($C^{(i)}$ is constant, $C^{(o)}$ varies); IV, asymmetric anion distribution ($C^{(o)}$ is constant, $C^{(i)}$ varies); S, symmetric anion distribution ($C^{(o)} = C^{(i)}$); MM, simple Michaelis-Menten fit; MS, Michaelis-Menten fit with self-inhibition; A, asymmetry factor ($E^{(o)}/E^{(i)}$ when $C^{(o)} = C^{(i)}$).

*OV and S data combined.

dependent on cell volume, in accordance with the results of Funder and Wieth (1976).

As shown in the Appendix, the outside saturation of the transport system at a fixed intracellular anion concentration can be described according to the ping-pong model by a simple Michaelis-Menten–like kinetics with a maximum flux, $J_{max}^{eff,o}$ (mol/[cm^2·s]), and a half-saturation constant, $K_{1/2}^{o}$ (mM). The experiments show, however, that the increase in unidirectional flux is less than expected from the simple Michaelis-Menten equation at $C^{(o)} > \sim 20$ mM in most experiments (Figs. 3 and 5). The phenomenon was not incorporated in the ping-pong model. We illustrate the

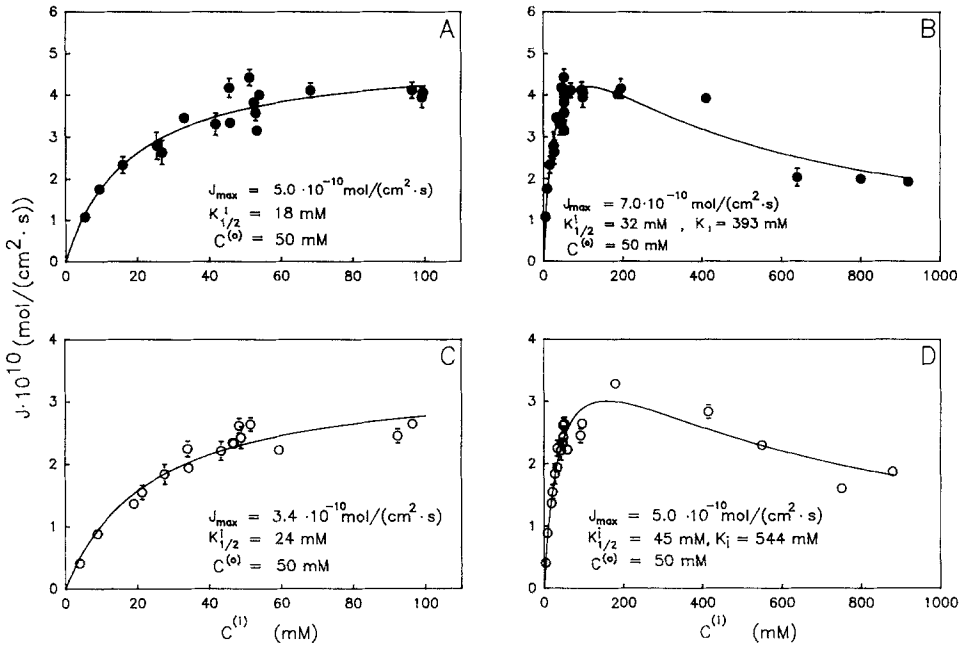

FIGURE 6. Bicarbonate (*A* and *B*) and chloride (*C* and *D*) self-exchange (0°C, pH 7.8) in resealed red cell ghosts under conditions of a constant extracellular anion concentration of 50 mM and variation of the intracellular anion concentration. For $C^{(i)}$ = 6–100 mM (*A* and *C*) the curve was drawn according to simple Michaelis-Menten–like kinetics. For $C^{(i)}$ = 6–900 mM (*B* and *D*) self-inhibition was included in the curve-fitting procedure. Sucrose was used to maintain equal external and internal tonicity.

deviation from ideality by performing two fitting procedures: in method 1, Eq. A5 was fitted to experimental data obtained in the concentration range 1–25 mM (bicarbonate, Fig. 2; chloride, Fig. 4); in method 2, Eq. A5 was fitted to the experimental data in the whole concentration range (bicarbonate, Fig. 3; chloride, Fig. 5). The results of the two analyses for bicarbonate and chloride are summarized in Table I. It appears that in all eight experimental series $J_{max}^{eff,o}$ and $K_{1/2}^{o}$ are both lowered by use of method 2. Note that in both methods the $J_{max}^{eff,o}$ values are significantly higher in bicarbonate experiments than in chloride experiments,

whereas the $K^{\circ}_{1/2}$ values are higher in chloride experiments. The table also shows that the results obtained with red blood cells and red cell ghosts under comparable experimental conditions are similar for both anions.

(b) Extracellular anion concentration is constant; cell anion concentration varies. The experiments were carried out with resealed red cell ghosts. The extracellular chloride or bicarbonate concentration was held constant at 50 mM and the intracellular concentration was varied between 6 and 920 mM (bicarbonate) and 6 and 880 mM (chloride) with sucrose as osmotic active substituent. The intracellular anion concentration used in plots of flux vs. $C^{(i)}$ was corrected in case of an osmotic difference

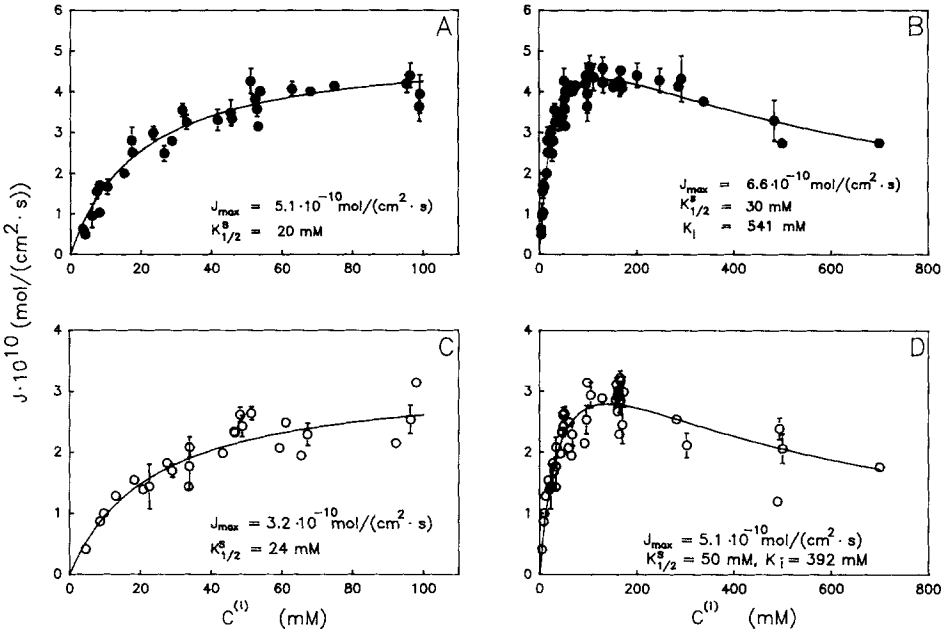

FIGURE 7. Bicarbonate (*A* and *B*) and chloride (*C* and *D*) flux (0°C, pH 7.8) in resealed ghosts under a symmetric ($C^{(i)} = C^{(o)}$) variation of the anion concentration. The abscissa depicts the intracellular anion concentration that is used to calculate the flux. For C = 1–100 mM (*A* and *C*) the curve was drawn according to simple Michaelis-Menten–like kinetics. For C = 1–700 mM (*B* and *D*) self-inhibition was included in the curve-fitting procedure. Sucrose was used to adjust cell volume at $C < 100$ mM.

between wash medium and flux medium. In the calculations we assumed that the ghost cells behaved as perfect osmometers ($V^{(i)} \cdot C^{(i)}/A$ is constant; i.e., the flux needs no correction). The results from the two asymmetric experimental series with bicarbonate and chloride are depicted in Fig. 6, and the results of the fitting procedure are summarized in Table I. We see that the bicarbonate and chloride self-exchange fluxes saturate as the intracellular anion concentration increases to ~200 mM and decrease at higher concentrations, suggesting that self-inhibition is related to the cytoplasmic side of the membrane for both anions. We performed two

analyses of the data in the concentration ranges 6–100 mM (bicarbonate and chloride), 6–920 mM (bicarbonate), and 6–880 (chloride). If Eq. A5 (see Appendix) is used for curve fitting to the experimental data obtained in the concentration range 6–100 mM, $J_{max}^{eff,i}$ for bicarbonate is 0.50 nmol/(cm^2·s) and $K_{1/2}^{i}$ is 18 mM (Fig. 6 *A*). Inclusion of intracellular self-inhibition in the ping-pong model (Eq. A15, Appendix) increases $J_{max}^{eff,s}$ and $K_{1/2}^{i}$ to 0.70 nmol/(cm^2·s) and 32 mM, respectively. The estimated equilibrium constant for intracellular noncompetitive inhibition is 393 mM (Fig. 6 *B*). The chloride data give $J_{max}^{eff,i}$ = 0.34 nmol/(cm^2·s) and $K_{1/2}^{i}$ = 24 mM in the low concentration range (Fig. 6 *C*). Using Eq. A15 yields $J_{max}^{eff,i}$ = 0.50 nmol/(cm^2·s) and $K_{1/2}^{i}$ = 45 mM. The estimated equilibrium constant for intracellular noncompetitive inhibition is 544 mM (Fig. 6 *D*). Both fitting procedures reveal that $K_{1/2}^{i}$ for both

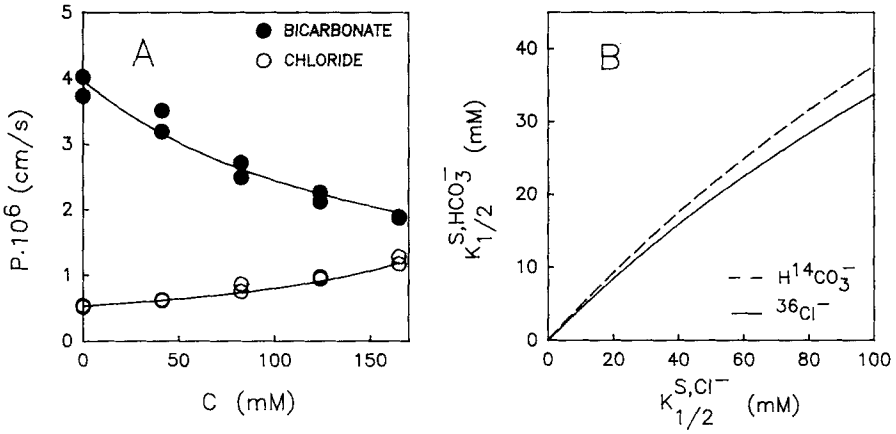

FIGURE 8. Bicarbonate (*filled circles*) and chloride (*open circles*) permeability as a function of the respective concentrations obtained in anion substitution experiments (*A*). (*B*) $K_{1/2}^{s}$ for bicarbonate versus $K_{1/2}^{s}$ for chloride as obtained from fitting to the tracer permeability data shown in *A* and Eq. A19*b*. Note the different scaling in *B*. The sum of the varied and symmetrically distributed bicarbonate and chloride concentrations was kept constant at 165 mM. See text and Appendix for further details.

anions is much higher than $K_{1/2}^{o}$ under similar experimental conditions for both anions.

(c) Intra- and extracellular anion concentrations are equal and vary simultaneously. The experiments were carried out with resealed red cell ghosts in the anion concentration range 5–700 mM. The unidirectional fluxes of both chloride and bicarbonate show saturation kinetics up to $C^{(o)} = C^{(i)} \approx 200$ mM (Fig. 7). We also see a decrease of self-exchange flux at C > 200 mM. The results of our analysis of the data in the concentration ranges 5–100 mM and 5–700 mM are summarized in Table I. Eq. A5 gives for bicarbonate (5–100 mM) $J_{max}^{eff,s}$ = 0.51 nmol/(cm^2·s), and the overall $K_{1/2}^{s}$ = 20 mM (Fig. 7 *A*). Fitting Eq. A15 to the whole data range (5–700 mM) gives $J_{max}^{eff,s}$ = 0.66 nmol/(cm^2·s) and $K_{1/2}^{s}$ = 30 mM. The equilibrium constant for intracellular noncompetitive self-inhibition is 541 mM (Fig. 7 *B*). The respective results for

chloride data are $J_{max}^{eff,s}$ = 0.32 nmol/(cm^2·s), $K_{1/2}^s$ = 24 mM (Eq. A5, 5–100 mM, Fig. 7 *C*) and $J_{max}^{eff,s}$ = 0.51 nmol/(cm^2·s), $K_{1/2}^s$ = 50 mM, and the equilibrium constant for intracellular noncompetitive self-inhibition is 392 mM (Eq. A15, 5–700 mM, Fig. 7 *D*).

Bicarbonate and chloride substitution experiments. It is also possible to obtain information about $K_{1/2}^s$ for both anions in substitution experiments where [^{14}C]HCO_3^- and $^{36}Cl^-$ transport are studied. Fig. 8 *A* shows the results of a substitution experiment where $C_{An} = C_{Cl^-} + C_{HCO_3^-}$ = constant = 165 mM, but the composition of the medium stepwise by 41.25 mM was varied from 165 mM KCl to 165 mM $KHCO_3$. Fig. 8 *A* depicts the tracer efflux permeability ($P = k \cdot [V_c^{(i)}/A_c]$) of bicarbonate (filled circles) and chloride (open circles) as a function of the respective concentrations. Bicarbonate tracer permeability decreased at increasing bicarbonate concentration (decreasing chloride concentration) and chloride tracer permeability increased with increasing chloride concentration (decreasing bicarbonate concentration). We note that the permeability of both anions in control cells decreased 15–20% after 24-h cold storage, in agreement with Wieth's (1979) results. The substitution experiments can be used to connect $K_{1/2}^s$ of the two anions (cf. Appendix). In Fig. 8 *B* $K_{1/2}^s$ for bicarbonate is depicted vs. values of $K_{1/2}^s$ of 0–100 mM for chloride. The results obtained with [^{14}C]HCO_3^- (dashed line) and ^{36}Cl (solid line) indicate that $K_{1/2}^s$ for chloride is at least twice as large as $K_{1/2}^s$ for bicarbonate (cf. Appendix, Eq. A19*b*).

DISCUSSION

The exchange of bicarbonate for chloride (the chloride or Hamburger shift) across the red cell membrane is an important step in the removal of CO_2 by the blood from the tissues to the lungs. The kinetics of self-exchange of the two anions are, except for a few studies (Wieth, 1979; Wieth and Brahm, 1980), investigated as chloride self-exchange, probably because it appears easier to use chloride as the probe for studies of the kinetics of monovalent inorganic anion transport in red cells. Hence, the currently accepted ping-pong model for monovalent inorganic anion transport has only been tested rigorously for chloride. A direct comparison of the asymmetry factors obtained for bicarbonate and chloride transport kinetics can provide a support to the proposed model. However, chloride data at 0°C give rise to a considerable scatter of the values of the asymmetry factor (see Knauf and Brahm, 1989). A possible explanation of the scatter is that different experimental procedures have been used. We have, therefore, performed both bicarbonate and chloride experiments to obtain results for both anions under identical experimental circumstances.

[^{14}C]HCO_3^- *Is Transported*

The control experiments in the present study make us conclude that the rate of [^{14}C] efflux represents bicarbonate transport across the red cell membrane as determined by [^{14}C]HCO_3^-. The conclusion is in agreement with the conclusion drawn by Wieth (1979), who studied bicarbonate transport under symmetric conditions at pH 8.7. As

our transport study is performed at pH 7.8, where the CO_2 concentration is approximately eight times higher and the spontaneous dehydration rate is several times faster, it is essential to resolve whether we indeed measure bicarbonate transport. Several lines of evidence support our conclusion. First, the linearity of the semilogarithmic plots of [^{14}C] efflux, as demonstrated in Fig. 1 *A*, shows that the decrease of intracellular radioactivity with time followed a monoexponential course, indicating that the overall rate coefficient is constant. Control experiments (not shown) show that the sum of intra- and extracellular radioactivity was constant during the efflux experiments. Hence, we conclude that any loss of radioactivity as $^{14}CO_2$ is negligible.

Second, the [^{14}C] efflux rate ($k = 0.074$ s^{-1}, $T_{1/2} = 9$ s) is much lower than the estimated $^{14}CO_2$ efflux rate[1] of 10^4 s^{-1}, and is of the same order of magnitude as the chloride efflux rate ($k^{Cl} = 0.050$ s^{-1}, $T_{1/2} = 14$ s). It is, therefore, not likely that the measured rate coefficient represents $^{14}CO_2$ efflux from the intracellular $^{14}CO_2$ pool. However, a small fraction of the intracellular radioactivity will be lost as $^{14}CO_2$. At pH 7.8 the equilibrium between CO_2 and HCO_3^- implies that ~5% of total CO_2 is physically dissolved CO_2. Therefore, we see a rapid efflux of the intracellular $^{14}CO_2$ pool that is in equilibrium with intracellular [^{14}C]HCO_3^- in the initial period of the experiment, as a downward displacement of the efflux curve that intersects with the ordinate at ~0.9 (e.g., Fig. 1 *A*). The initial rapid efflux of the labeled CO_2 pool is followed by a continuous and slow efflux of $^{14}CO_2$, which is produced by dehydration of labeled bicarbonate. The slow efflux of $^{14}CO_2$, however, contributes very little to the total efflux of radioactivity after inhibition of carbonic anhydrase by means of acetazolamide (cf. Methods). By maximum inhibition the time constant of the reaction is decreased ~10,000 times, so that 50% conversion takes >100 min, as determined for the spontaneous reaction at 0°C, pH 7.8 (based on the data of Magid and Turbeck, 1968). The contribution by the continuous and slow $^{14}CO_2$ efflux to the measured [^{14}C] efflux under conditions of self-exchange at 165 mM bicarbonate (0°C, pH 7.8) can be estimated from Fig. 1 *B*. [^{14}C] efflux is ~98.3% inhibited in the DIDS-treated cells, indicating that $^{14}CO_2$ (and [^{14}C]H_2CO_3) efflux is <2% of the total [^{14}C] efflux (assuming that DIDS inhibits bicarbonate transport by ~100%); that is, ~98% is efflux of [^{14}C]HCO_3^-. Under conditions with high cellular bicarbonate concentrations (≤920 mM) $T_{1/2}$ of [^{14}C]HCO_3^- efflux increases approximately four times, while $T_{1/2}$ of $^{14}CO_2$ is constant. Under such extreme conditions the $^{14}CO_2$ efflux may constitute a maximum of 6–7% of the measured [^{14}C] efflux.

The plots of Fig. 1 *B* further demonstrate the importance of inhibiting the intracellular carbon anhydrase. After the initial rapid loss of $^{14}CO_2$, the lack of acetazolamide inhibition of carbon anhydrase results in a continuous loss of $^{14}CO_2$ after a continuous cellular dehydration of [^{14}C]HCO_3^- (triangles and squares). If DIDS is present (triangles) the slope of the [^{14}C] efflux curve decreases and approaches

[1] The estimated rate coefficient, k s^{-1}, is calculated from the relation $k = P \cdot A_c / V_c^{(i)}$ using a permeability coefficient, P, of 0.4 cm/s for CO_2 diffusion in bimolecular lipid membrane (Gutknecht et al., 1977), and a ratio of cell water volume to membrane area ($V_c^{(i)}/A_c$) for red cells of $4.3 \cdot 10^{-5}$ cm (Wieth et al., 1974).

after ~40 s the slope of the plot of [^{14}C] efflux under conditions with inhibition by DIDS and acetazolamide (dashed line). In the absence of DIDS and acetazolamide (squares) the slope of the plot gradually changes too. After 8–10 s the slope is similar to the slope obtained with control cells treated with acetazolamide but not DIDS (circles), and after ~20 s the slope becomes even smaller. The paradox, that the rate coefficient for [^{14}C] efflux is slower under experimental conditions with uninhibited carbonic anhydrase (squares) than in control cells (circles), can be explained by the fact that CO_2 rapidly permeates the cell membrane and is converted to bicarbonate (or vice versa) at a very fast rate due to the presence of carbonic anhydrase in cells without acetazolamide. At time zero (whether or not DIDS and/or acetazolamide are present) ~99.5% of the $^{14}CO_2$ in the cells (~5% of total [^{14}C]) rapidly diffuses into the extracellular compartment, which is ~200 times larger than the cellular compartment. The $^{14}CO_2$ efflux creates an intracellular disequilibrium between $^{14}CO_2$ and [^{14}C]HCO_3^- and initiates an intracellular net dehydration of [^{14}C]HCO_3^- to H_2O and $^{14}CO_2$, which is very fast in cells not treated with acetazolamide. The major fraction of the continuously produced $^{14}CO_2$, ~99.5%, also diffuses out of the cells. As the intra- and extracellular concentrations of $^{14}CO_2$ increase and the intracellular concentration of [^{14}C]HCO_3^- decreases with time, net dehydration of cellular [^{14}C]HCO_3^- and the efflux of $^{14}CO_2$ decrease and the efflux of [^{14}C]HCO_3^- becomes more dominating. When intracellular equilibrium between [^{14}C]HCO_3^- and $^{14}CO_2$ is restored (after ~10 s) no net efflux of $^{14}CO_2$ occurs and the slopes of the two curves become equal, although carbonic anhydrase is inhibited in only one of the two experiments. In cells with active carbonic anhydrase a further loss of cell [^{14}C]HCO_3^- next induces a net hydration of cell $^{14}CO_2$ to [^{14}C]HCO_3^-. The removal of intracellular $^{14}CO_2$ is compensated for by influx of extracellular $^{14}CO_2$. The reentry of $^{14}CO_2$ and intracellular hydration to [^{14}C]HCO_3^- give rise to a slower efflux rate after ~10 s in cells that are not inhibited by acetazolamide.

The Asymmetry of Chloride and Bicarbonate Transport

The study of chloride self-exchange by Gunn and Fröhlich (1979) shows that the transport system has an intrinsic, functional asymmetry, as the apparent internal affinity to chloride is ~15 times less than the apparent external affinity. The authors concluded that the kinetics of anion exchange were compatible with the concept of the reciprocating or ping-pong model as described elsewhere (Knauf, 1979; Knauf et al., 1984; Fröhlich and Gunn, 1986; Passow, 1986; this study). A major simplification of the kinetics in the model comes from the experimental evidence that chloride self-exchange is ~$2.5 \cdot 10^4$ times larger than the conductive flow at body temperature (Brahm, 1977; Hunter, 1977).[2] The ping-pong model incorporates the extremely low net flow of anions by assuming that anion translocation takes place exclusively after

[2] We are not aware of any studies of Cl^- conductance at 0°C, or of the temperature dependence of the Cl^- conductance in human red cells. The chloride exchange decreases by ~200 times from 38 to 0°C (Brahm, 1977), and the simplification of the model still applies at 0°C even if the temperature dependence is very low. If one assumes that the temperature dependence of the conductance is zero, the chloride self-exchange should be at least 100 times larger than the conductive flow at 0°C.

formation at one side of the membrane of a transport site anion complex that reciprocates to the other side of the membrane with a subsequent liberation of the anion from the transport site (cf. Eq. A1) (for a discussion of the anion conductance mode, "slippage," or "tunneling," see Fröhlich, 1984).

The characterization of the functional asymmetry of anion transport using the asymmetry factor is based on the presumption that the ping-pong model (simple or modified) indeed describes anion exchange flux. It should be noted, however, that any functional asymmetry of the anion transporter can be demonstrated independent of a specific model (see below).

The asymmetry of capnophorin is in the ping-pong model represented by the asymmetry factor, A, the ratio of unloaded sites ($E^{(o)}/E^{(i)}$) under conditions with $C^{(i)} = C^{(o)}$. A can be determined by several combinations of experimental procedures (see Appendix). The model predicts that anion flux increases by an increase of anion concentration on either one or both sides of the membrane. However, studies (e.g., Dalmark, 1976; Funder and Wieth, 1976; Wieth, 1979; Knauf and Mann, 1986; this study) show a decline of anion flux at high intracellular anion concentrations, a phenomenon that was interpreted in terms of anion binding to a modifier site causing a noncompetitive self-inhibition (Dalmark, 1976). Knauf and Mann (1986) suggested that self-inhibition for chloride transport takes place predominantly on the cytoplasmic side of the membrane, and their results agree with our study demonstrating that chloride and bicarbonate flux decline at intracellular concentrations >200 mM. We therefore include an intracellular modifier site in the model as the simplest adjustment of the model to the experimental data. A decrease of flux caused by an intracellular, one-site, noncompetitive self-inhibition may have a pronounced effect on the determination of the "true" half-saturation constants and maximum fluxes if one uses the simple, unmodified ping-pong model at concentrations <100 mM, and may cause a significant error in calculation of the asymmetry factor.

We extended the concentration range under study up to ~ 1 M. This makes it possible to demonstrate the effect of self-inhibition on the determination of the asymmetry factor, and we fitted both the simple and the modified ping-pong models to the experimental results in our analysis.

We determined A for bicarbonate and chloride transport, respectively, by measuring the outside apparent affinity, $K^{o}_{1/2}$ (mM), under conditions of constant and high intracellular bicarbonate or chloride concentration and a varying extracellular concentration, and the overall apparent affinity, $K^{s}_{1/2}$ (mM), under conditions of varying intra- and extracellular concentrations that are kept equal (Eq. A11).

$C^{(i)}$ Is Constant; $C^{(o)}$ Varies

The extracellular anion concentration was varied in four series with constant intracellular anion concentrations. As two values of the outside half-saturation constant, $K^{o}_{1/2}$, were determined for each experimental series, we determined eight values of $K^{o}_{1/2}$ for each anion. The values are in the range 1.2–2.4 mM for bicarbonate and 1.4–2.6 mM for chloride transport (cf. Table I). We made two curve fits for each series of experiments (cf. Methods), one fit by using the simple Michaelis-Menten equation in the total experimental concentration range, and the other by using the equation in the range 1–25 mM, taking into account that the experiments show a

maximum flux at $C^{(o)} \approx 15$–30 mM and a small decrease at $C^{(o)} > 30$ mM. The increase of anion efflux as the anion concentration in the efflux medium is raised from 1 to ~10 mM is explained in terms of the ping-pong model as an increase of "recruitment" of external transport sites to the inside of the membrane that increases the number of internal anion transport site complexes and thereby the anion efflux rate.

The small decline in anion flux at higher extracellular concentrations (Figs. 3 and 5) may be a direct extracellular effect of anions on the transport system, for example, by binding to an extracellular modifier site with a high affinity for bicarbonate and chloride. However, the external self-inhibition must be partial because the curve approaches a constant level above zero. A partial self-inhibition suggests either a heterogeneity of the capnophorin molecules, of which a fraction can be inhibited by external anions, or a "slow down" of the transport rate by binding of an anion to the external modifier site. We attempted to fit a ping-pong model with an extracellular modifier site (causing partial inhibition) to our experimental data. The model included four free parameters ($K^{o}_{1/2}$, $J^{eff,o}_{max}$, K_i, and a fourth parameter [< 1] that represents the incomplete inhibition), but the fitting to the experimental data was poor. We therefore decided to use the two procedures of curve fitting in two concentration ranges. The general result is that our analysis (Table I) shows higher values of $K^{o}_{1/2}$ and $J^{eff,o}_{max}$ for the concentration range 1–25 mM, as compared with the fitting values obtained for the total experimental concentration range.

The local maximum phenomenon (Figs. 3 and 5) has also been found for chloride transport by Knauf and Mann (1986). They suggested that the phenomenon is related to variations of ionic strength in the efflux media as potassium/sodium chloride was replaced by a nonelectrolyte at low concentrations. It is possible that we also see an effect of ionic strength on anion transport in our experiments since the only anion present was either Cl^- or HCO_3^-. The possible effects of ionic strength and partial self-inhibition underline the fact that the parameters of the fitting procedures should be characterized as apparent.

The variation of the external anion concentrations may also have another indirect effect on the appearance of the saturation curves. Because the chloride conductance is >100 times larger than the potassium conductance, the membrane potential in chloride experiments is close to the equilibrium potential for chloride and varies substantially in such experiments. The generally accepted concept that the membrane potential does not affect the electrosilent, tightly coupled chloride exchange in intact red cells and ghosts has recently been questioned by Grygorczyk et al. (1987). Their study of mouse band 3 expression in oocytes shows that the electrosilent chloride exchange was increased 1.5 times as the membrane potential was changed from −20 to −70 mV. The authors suggested that the potential-dependent change of anion transport was due to a redistribution of the anion-loaded transport sites. We find it unlikely that the unidirectional chloride efflux in our study is significantly affected by the membrane potential. As shown in Fig. 5 *D*, the chloride efflux is constant by a variation of only the extracellular chloride concentration between 25 and 235 mM. The membrane potential decreases by ~50 mV, and we find it unlikely that a possible effect of the membrane potential should be counterbalanced by other

mechanisms such as ionic strength and increased binding of chloride to the transport system.

The net bicarbonate permeability has been estimated indirectly at 37°C (pH 7.5) to be $5.5 \cdot 10^{-7}$ cm/s (Knauf et al., 1977) as compared with the apparent permeability for bicarbonate self exchange of $1.5 \cdot 10^{-4}$ cm/s (Wieth and Brahm, 1980). We do not know the magnitude of the bicarbonate conductance at 0°C and its possible role in determining the membrane potential. If, however, conductive flow of $[^{14}C]HCO_3^-$ is significant, it is not likely that bicarbonate efflux should remain constant in our experiments (Fig. 3 *D*) where the membrane potential varied ~50 mV.

It is also unlikely that a net flow of K^+ and Cl^- or HCO_3^- plays an important role in our study. Net efflux of KCl increases at low extracellular Cl^- concentrations (see Jones and Knauf, 1985). However, at the lowest extracellular chloride concentrations used in the present study (1 and 2 mM) net chloride efflux from resealed ghosts, as estimated from chloride titration of the efflux media (<3% of the total efflux; data not shown), was not significant.

The effect of a change in internal pH should be considered in the asymmetric experiments. pH changes as the chloride gradient across the membrane is varied according to $C^{(i)}_{H^+}/C^{(o)}_{H^+} = C^{(o)}_{Cl^-}/C^{(i)}_{Cl^-}$. If cells with a higher chloride content at pH 7.8 are suspended in a low chloride medium at the same pH value, the cells alkalize and the medium acidifies. The buffer capacity in the ghosts is small compared with the buffer capacity of the efflux medium. Hence, the cells alkalize, whereas the pH in the efflux medium remains almost constant during the efflux experiment. The intracellular alkalinization in resealed ghosts is rapid and approaches the expected value from the chloride distribution ratio as measured using fluorescence spectrometry and the pH-sensitive dye BCECF (data not shown).

The intracellular alkalinization is, however, not a likely cause of the local maximum phenomenon, because the intracellular pH value is increased less than two pH units. Funder and Wieth's study (1976) of pH dependence of chloride flux in intact red blood cells and resealed ghosts under symmetric conditions at 0°C shows that the anion efflux is constant in the range $pH^{(i)} = pH^{(o)}$ 7–10 for resealed ghosts.

In RBC that are strongly buffered by hemoglobin, a slight extracellular alkalinization was seen in weakly buffered media in experiments with low extracellular chloride. The effect was completely abolished by 1 mM intracellular acetazolamide, underlining the role of carbon dioxide and bicarbonate in pH equilibration. Control experiments showed, however, that bicarbonate removal by N_2 bubbling had no effect on the chloride efflux rate in low chloride media (1–2 mM).

Although intracellular noncompetitive inhibition was not included in the fitting procedures, the fitting results may be affected by this phenomenon. If one assumes that the decline in anion flux at increasing and high intracellular concentrations is caused by a one-site, intracellular, noncompetitive self-inhibition, the estimated outside maximum flux, $J^{eff,o}_{max}$ must be corrected for this effect. As the self-inhibition is assumed to be noncompetitive and unaffected by the orientation of the transport site, the estimated outside half-saturation constants, $K^o_{1/2}$, are not affected by the phenomenon. However, the values of $J^{eff,o}_{max}$ are reduced because a certain number of transport proteins are inactivated by the intracellular binding of anions to the modifier site. The "true" hypothetical $J^{eff,o}_{max}$ can be calculated from the obtained $J^{eff,o}_{max}$ by multiplica-

tion with $(1 + C/K_i)$, where C designates the fixed intracellular anion concentration and $1/K_i$ the equilibrium constant for binding of the anion to the intracellular modifier site.

It can be shown (see Appendix) that the theoretical value of $K^o_{1/2}$ increases with increasing internal anion concentration and reaches a maximum value, $K^o_{1/2max}$, that should be obtained under conditions where all the intracellularly facing transport sites are loaded. A rough estimate from our results indicates that $K^o_{1/2max}$ for bicarbonate transport is ~3.0 mM and ~3.1 mM for chloride at 0°C, pH 7.8 ($C^{(o)}$ = 1–25 mM). Studies of chloride self-exchange at 0°C (Gunn and Fröhlich, 1979; Fröhlich, 1982; Hautmann and Schnell, 1985) show $K^o_{1/2max}$ values from 1.5 to 6.2 mM with a mean of 3.8 mM (Table 1 in Knauf and Brahm, 1989). Hence, the outside apparent affinities of the transport system to bicarbonate and chloride differ but little.

$C^{(i)}$ and $C^{(o)}$ Vary Simultaneously

Fig. 7, *B* and *D*, shows that chloride and bicarbonate transport under conditions of symmetric distribution of the anion concerned ($C^{(i)} = C^{(o)}$) reach an observed maximum flux at C = 100–200 mM, and gradually decline with a further increase of the concentrations to 700 mM. Values of $K^s_{1/2}$ for chloride in the range 21–65 mM have been reported (Brazy and Gunn, 1976; Dalmark, 1976; Fröhlich, 1982; Hautmann and Schnell, 1985; Knauf and Brahm, 1989). Our two values (24 and 50 mM, cf. Table I) show the effect of including simple self-inhibition in the ping-pong model.

Wieth's study (1979) of bicarbonate transport was carried out under self-exchange conditions with resealed ghosts at pH 8.7, 0°C. He reports an observed half-maximum exchange flux at 10 mM. By curve fitting including self-inhibition, he found a $K^s_{1/2}$ of 20 mM and a K_i of 600 mM. We show here that bicarbonate transport can be studied at a more physiological pH value. Excluding self-inhibition (method 1) we get a $K^s_{1/2}$ of 20 mM. By including self-inhibition (method 2) we get $K^s_{1/2}$ = 30 mM and K_i 541 mM that should be compared with the respective values of 20 and 600 mM obtained by Wieth (1979). We cannot exclude that the differences are caused in part by a pH dependence of bicarbonate transport.

Initially we assumed that the low affinity of bicarbonate to the postulated modifier site made it possible to determine the asymmetry of bicarbonate transport without correction for self-inhibition. Dalmark's study (1976) of halide self-exchange under symmetric conditions showed an overall self-inhibition binding constant of 335 mM for chloride and 585 mM for bicarbonate. At a given anion concentration self-inhibition should be less for bicarbonate than chloride and the bicarbonate flux, therefore, should be closer to the "true" uninhibited flux according to the simple Michaelis-Menten–like kinetics (Eq. A5). The results of this study (cf. Table I), however, show that the degree of self-inhibition does not differ significantly for chloride and bicarbonate transport, as the mean values of the estimated intracellular inhibition constants are 467 ± 50 mM for bicarbonate and 458 ± 69 mM for chloride. It should be noted that the values of Dalmark's (1976) and Wieth's (1979) studies for chloride and bicarbonate binding to the modifier site were obtained under symmetric conditions and from fewer points (cf. Fig. 3 in Dalmark, 1976, and Fig. 9

in Wieth, 1979) than in our study, and were not calculated by means of an advanced statistical program such as we used.

In general all the fitting results for both anions are very similar to the results obtained in the asymmetric series with $C^{(o)}$ = 50 mM and a varied intracellular concentration. The results indicate that 50 mM external chloride or bicarbonate saturates the transport system in accordance with the results obtained in the asymmetric series with a constant high intracellular and a varied extracellular anion concentration.

The Asymmetry Factor A

According to the ping-pong model the asymmetry factor A can be calculated if, for example, $K^s_{1/2}$ and $K^o_{1/2}$ are known. The determinations of $K^o_{1/2}$ and $K^s_{1/2}$ that are summarized in Table I provide us with a value of A in the range of 0.06–0.12 for

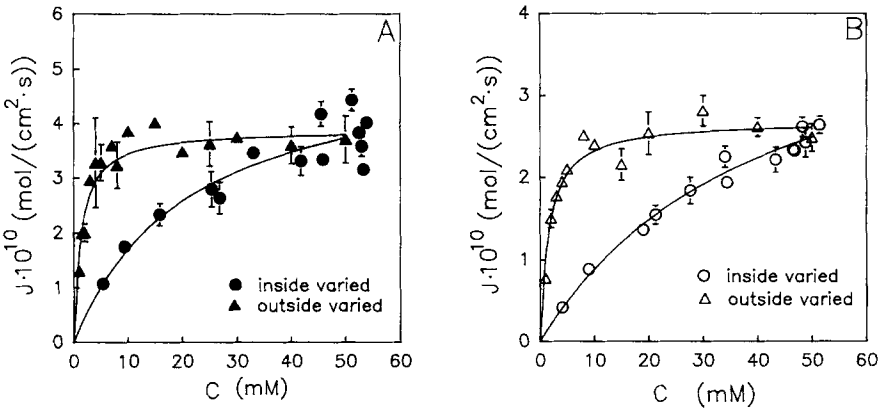

FIGURE 9. Asymmetry of bicarbonate (A) and chloride (B) self-exchange flux (0°C, pH 7.8) in resealed ghosts demonstrated under conditions of (a) $C^{(i)}$ = 50 mM and $C^{(o)}$ = 1–50 mM (▲ and △), and (b) the reversed situation $C^{(o)}$ = 50 mM and $C^{(i)}$ = 1–50 mM (● and ○). Sucrose was used to keep internal and external tonicity equal.

bicarbonate and 0.05–0.12 for chloride. It should be noted here that the generally used asymmetry factor for chloride transport (0.064, Gunn and Fröhlich, 1979) represents the lower extreme of a range up to 0.32 with a mean of 0.15 obtained from different studies (Gunn and Fröhlich, 1979; Fröhlich, 1982; Hautmann and Schnell, 1985; Knauf and Brahm, 1989).

Basically A has been calculated by use of results from experiments with $C^{(i)}$ = constant, $C^{(o)}$ varied, and $C^{(i)} = C^{(o)}$ varied. Hence, the interpretation that the transport system is functionally asymmetric is based on the validity of the ping-pong model. A more direct approach to illustrating the asymmetry, as was also indicated by Gunn and Fröhlich (1979), is as follows: assuming only that anion influx and efflux are equal, the functional asymmetry can be demonstrated in a model-independent way if two exactly inverted asymmetric experimental series are carried out. Fig. 9 shows the results of experiments with C_{An} = 50 mM and a *trans*-concentration varied

between 1 and 50 mM. The results illustrate the functional asymmetry of the anion transporter. The anion transporter has the highest apparent affinity for both chloride and bicarbonate on the outward-facing side of the membrane. If, for example, the concentration distribution of bicarbonate is reversed from 50 mM outside and 5 mM inside to 5 mM outside and 50 mM inside, the bicarbonate flux across the membrane is increased about three times. A can also be calculated from these two asymmetric series using the ping-pong model and the half-saturation constants from Table I: $A = (1/C^{(o)} + 1/K^{i}_{1/2})/(1/C^{(i)} + 1/K^{o}_{1/2})$. For both anions A is 0.11 if method 1 is used and 0.064 if method 2 is used. The values support the ping-pong model because the calculated values of A are almost the same as when $K^{o}_{1/2}$ and $K^{s}_{1/2}$ are used (see above), and A is the same for the two anions.

Bicarbonate and Chloride Substitution Experiments

The substitution experiments show (Fig. 8) that bicarbonate has a higher apparent overall affinity to the transport system, as also shown by Gunn et al. (1973) and Wieth (1979). It is, however, not possible to determine a single value of the ratio between the affinities as the two studies may suggest. Nor is it possible to determine an absolute value of $K^{s}_{1/2}$ in the substitution experiments. However, a value of $K^{s}_{1/2}$ for one of the anions can be calculated if $K^{s}_{1/2}$ for the other anion has been determined in "single anion experiments" with $C^{(i)}$ and $C^{(o)}$ equal and varied. The ratio depends on the magnitude of $K^{s}_{1/2}$ (Fig. 8 *B*, cf. Eqs. A20*a* and A20*b* in the Appendix). The initial slope of the curves of Fig. 8 *B* demonstrate that the ratio $K^{s}_{1/2}$ (Cl^-)/$K^{s}_{1/2}$ (HCO_3^-) is at least 2. The ratio increases with an increasing $K^{s}_{1/2}$, indicated in Fig. 8 *B* by a value of 3 at $K^{s}_{1/2}$ (Cl^-) = 100 mM.

The results of the substitution experiments are in favor of the results in Table I for $K^{s}_{1/2}$ of chloride and bicarbonate obtained by means of the modified ping-pong model. $K^{s}_{1/2}$ for chloride is 50 ± 10 mM (SE). Using this value, Fig. 8 *B* reveals that $K^{s}_{1/2}$ for bicarbonate is ~20 mM, which is close to the value of $K^{s}_{1/2}$ for bicarbonate in Table I (30 ± 3 mM [SE]). It should be noted that self-inhibition was not included in the analysis of the results of the substitution experiments. It was assumed that self-inhibition was independent of the anion composition of the media, as the K_i values for the two anions are similar (cf. Table I). The conclusion arising from the substitution experiments is that this type of experiment provides us with a helpful test of the ping-pong model of anion exchange, though an exact ratio of the apparent overall affinities of the anions to the transport system cannot be obtained.

Conclusion

From this study we conclude that the asymmetry of the transport system essentially remains unchanged independent of whether chloride or bicarbonate is transported, in agreement with the currently accepted ping-pong model of anion transport. We further conclude that the asymmetry factor A depends on whether or not self-inhibition is included in the model, and on which extracellular concentration range is studied in experiments with a fixed intracellular concentrations. We here show that A for both anions is ~0.06 if self-inhibition is included in the ping-pong model and results from the total extracellular concentration range are used in the analyses. A is ~0.12 for both anions if self-inhibition is ignored and the varied intracellular

concentration ranges are limited to 5–100 mM and the extracellular ranges are limited to 1–25 mM in experiments with fixed intracellular concentrations. Other values of A between 0.06 and 0.12 can be obtained by combining results from analyses where (*a*) self-inhibition is ignored and the total extracellular concentration range is used in experiments with fixed intracellular concentrations, and (*b*) self-inhibition is included and a limited extracellular concentration range in experiments with fixed intracellular concentrations is used in the analyses.

This study underlines the importance of defining the experimental conditions under which A is determined, and indicates the necessity of calling A apparent. Our results do not permit us to conclude whether the different values of $K^{o}_{1/2}$ reflect the influence of extrinsic factors such as ionic strength on the experimental determination of a "true" outside half-saturation constant or reflect a more complex interaction between anion and transport systems than assumed in the ping-pong model. An important observation is that under identical experimental conditions A_{app} is similar for chloride and bicarbonate transport, in agreement with the prediction arising from the ping-pong model.

APPENDIX

The Asymmetry Factor A

The kinetics of the reciprocating or "ping-pong" model have been derived by means of rate coefficients for the different reaction steps (see Knauf, 1979; Knauf et al., 1984; Fröhlich and Gunn, 1986; Passow, 1986). We here show that the parameters that describe the saturable anion transport process under self-exchange conditions can be obtained by use of a general solution for a transport process with three reaction steps (Britton, 1964).

In the ping-pong model the transport sites face either inward (unloaded $[E^{(i)}]$ or loaded with an anion $[AnE^{(i)}]$), or outward (unloaded $[E^{(o)}]$ or loaded $[AnE^{(o)}]$). Anion transport across the membrane is restricted and takes place only after binding to E, and E is assumed not to perform a conformational change without complexing with an anion. Hence, the conductive pathway, which is either a return of an empty transport site or anion translocation without a conformational change of the transport protein, is neglected as net chloride flux is $\sim 2.5 \cdot 10^4$ times lower than the exchange flux (38°C; Brahm, 1977; Hunter, 1977). The reaction scheme of the model is:

$$An^{(i)} + E^{(i)} \underset{k_{-1}}{\overset{k_1}{\rightleftarrows}} AnE^{(i)} \underset{k_{-2}}{\overset{k_2}{\rightleftarrows}} AnE^{(o)} \underset{k_{-3}}{\overset{k_3}{\rightleftarrows}} An^{(o)} + E^{(o)} \tag{A1}$$

The unidirectional efflux of solute is:

$$J^{eff} = D \cdot C_{An}{}^{(i)} \cdot C_E{}^{(i)}$$

where C denotes the concentration, and

$$D = k_1 \cdot k_2 \cdot k_3 / (k_2 \cdot k_3 + k_{-1} \cdot k_3 + k_{-1} \cdot k_{-2}) \tag{A2}$$

as derived by Britton (1964) (D in Eq. A2 is equal to 1/b in Fröhlich and Gunn, 1986). If one assumes that the binding/dissociation steps (k_1 and k_{-1}, k_3 and k_{-3}) proceed so rapidly that translocation (k_2 and k_{-2}) becomes the rate-limiting step of the transport process, one gets the expression of the simple model shown by Knauf et al. (1984). The NMR study by Falke et al. (1985) supports the conclusion that translocation is rate limiting.

$C_E^{(i)}$ is eliminated using conventional methods that introduce the total concentration of transporter, T, and the three equilibrium constants, so one obtains:

$$J^{eff} = T \cdot D \cdot C_{An}^{(i)} / (1 + C_{An}^{(i)} \cdot K_1 + C_{An}^{(i)} \cdot K_1 \cdot K_2 + C_{An}^{(i)} \cdot K_1 \cdot K_2 \cdot K_3 / C_{An}^{(o)}) \quad \text{(A3)}$$

which is simplified by introduction of $S = K_1 \cdot K_2 + K_1$, and $A = K_1 \cdot K_2 \cdot K_3$ (the nth equilibrium constant K_n is defined as the ratio k_n/k_{-n}):

$$J^{eff} = T \cdot D \cdot C_{An}^{(i)} / (1 + C_{An}^{(i)} \cdot S + C_{An}^{(i)} \cdot A / C_{An}^{(o)}) \quad \text{(A4)}$$

If (*a*) $C_{An}^{(o)}$ varies and $C_{An}^{(i)}$ is constant, (*b*) $C_{An}^{(o)}$ is constant and $C_{An}^{(i)}$ varies, and (*c*) $C_{An}^{(o)} = C_{An}^{(i)}$ varies, Eq. A4 reduces to a Michaelis-Menten–like expression:

$$J = J_{max} \cdot C_{An} / (K_{1/2} + C_{An}) \quad (\text{mol}/[\text{cm}^2 \cdot \text{s}]) \quad \text{(A5)}$$

Under the three experimental conditions the maximum unidirectional efflux, J_{max}^{eff}, and the half-saturation constant, $K_{1/2}$ are:

(a) $C_{An}^{(o)}$ varies, $C_{An}^{(i)}$ is constant:

$$J_{max}^{eff,o} = T \cdot D / (S + 1/C_{An}^{(i)}) \quad (\text{mol}/[\text{cm}^2 \cdot \text{s}]) \quad \text{(A6}a\text{)}$$

$$K_{1/2}^{o} = A / (S + 1/C_{An}^{(i)}) \quad (\text{mM}) \quad \text{(A6}b\text{)}$$

At saturating (infinite) intracellular anion concentration Eq. A6*b* becomes:

$$K_{1/2}^{o} = K_{1/2,max}^{o} = A/S \quad (\text{mM}) \quad \text{(A6}c\text{)}$$

(b) $C_{An}^{(o)}$ is constant, $C_{An}^{(i)}$ varies:

$$J_{max}^{eff,i} = T \cdot D / (S + A/C_{An}^{(o)}) \quad (\text{mol}/[\text{cm}^2 \cdot \text{s}]) \quad \text{(A7}a\text{)}$$

$$K_{1/2}^{i} = 1/(S + A/C_{An}^{(o)}) \quad (\text{mM}) \quad \text{(A7}b\text{)}$$

At saturating (infinite) extracellular anion concentration Eq. A7*b* becomes:

$$K_{1/2}^{i} = K_{1/2,max}^{i} = 1/S \quad (\text{mM}) \quad \text{(A7}c\text{)}$$

(c) $C_{An}^{(o)} = C_{An}^{(i)}$ varies:

$$J_{max}^{eff,s} = T \cdot D/S \quad (\text{mol}/[\text{cm}^2 \cdot \text{s}]) \quad \text{(A8}a\text{)}$$

$$K_{1/2}^{s} = (A + 1)/S \quad (\text{mM}) \quad \text{(A8}b\text{)}$$

The three half-saturation constants are related by:

$$K_{1/2}^{s} = (A + 1)/S = A/S + 1/S = K_{1/2,max}^{o} + K_{1/2,max}^{i} \quad (\text{mM}) \quad \text{(A9)}$$

A is the asymmetry factor defined by Knauf (1984) as:

$$A = E^{(o)}/E^{(i)}, \text{ for } C_{An}^{(i)} = C_{An}^{(o)} \quad \text{(A10)}$$

A can be determined by several combinations of the half-saturation constants. Combination of Eqs. A6*b* and A8*b* gives:

$$A = (K_{1/2}^{s}/C_{An}^{(i)} + 1)/(K_{1/2}^{s}/K_{1/2}^{o} - 1) \quad \text{(A11)}$$

as also derived by Knauf and Brahm (1989). Combining Eqs. A6*c* and A7*c* yields:

$$A = K_{1/2,max}^{o}/K_{1/2,max}^{i} \quad \text{(A12)}$$

Values of A different from 1 indicate that the ratio of the true internal and external affinities for the anion and/or the ratio of the two translocation rates for the loaded protein differ from unity as $A = K_1 \cdot K_2 \cdot K_3$.

Eq. A6*b* shows that the value of $K^{o}_{1/2}$ depends on which fixed cell anion concentration is used in the experiments as shown experimentally by Gunn and Fröhlich (1979). This is an important point to take into account in comparing of $K^{o}_{1/2}$ values obtained in different experiments and studies. Eq. A7*b* shows that $K^{i}_{1/2}$ correspondingly is related to the external anion concentration.

Modification of the Ping-Pong Model

The simple ping-pong model does not apply to experimental results obtained at high anion concentrations where the unidirectional anion flux decreases by raising the anion concentration (self-inhibition). Self-inhibition can be accounted for by introduction of a modifier site (Dalmark, 1976). We assume that binding of an anion to an internal modifier site (which results in inhibition of anion transport, with K_i denoting the reciprocal equilibrium constant for anion binding to the site) is independent of binding of an anion to the transport site and the position of the transport site (noncompetitive inhibition). Inclusion of self-inhibition in the simple ping-pong model can be done in the following way:

$$An^{(i)} + E \rightleftarrows EAn^{(i)} \tag{A13}$$

E denotes all unloaded and loaded forms of the transport protein in the simple ping-pong model ($C_E = T$ if $C^{(i)}_{An} = 0$). Under equilibrium conditions we have:

$$C_E = K_i \cdot C^{(i)}_{EAn}/C^{(i)}_{An} = T - C^{(i)}_{EAn} = T - C_E \cdot C^{(i)}_{An}/K_i = T/(1 + C^{(i)}_{An}/K_i) \tag{A14}$$

C_E is the concentration of functional transport proteins and replaces T in Eq. A5. The intracellular noncompetitive inhibition therefore implies a modification of the simple Michaelis-Menten kinetics (Eq. A5) to:

$$J = J_{max} \cdot C_{An}/[(K_{1/2} + C_{An}) \cdot (1 + C^{(i)}_{An}/K_i)] \quad (\text{mol}/[\text{cm}^2 \cdot \text{s}]) \tag{A15}$$

Here C_{An} is the varied anion concentration (internal or external anion concentration with a fixed *trans*-concentration, or both if $C^{(i)}_{An} = C^{(o)}_{An}$ is varied). In experiments with constant cellular concentration (experimental condition 1) the expression of Eq. A5 still applies, as the internal noncompetitive inhibition only causes a constant reduction of the hypothetical uninhibited maximum efflux, $J^{eff,o}_{max}$. In experiments with a varied cellular concentration (conditions 2 and 3), the unidirectional efflux declines at high concentrations and converges toward zero if the anion concentration increases infinitely (cf. Wieth and Bjerrum, 1983). The assymmetry factor still can be calculated using Eqs. A11 or A12.

Anion Substitution Experiments

In substitution experiments with two symmetrically distributed anions ($C_a = C^{(i)}_a = C^{(o)}_a$ and $C_b = C^{(i)}_b = C^{(o)}_b$) one can derive an extended version of Eq. A4:

$$J^{eff,s}(a) = T \cdot D \cdot C_a/[1 + C_a \cdot S(a) + A + C_b \cdot S(b)] \tag{A16}$$

Combining Eqs. A8*a*, A8*b*, and A16:

$$J^{eff,s}(a) = J^{eff,s}_{max}(a) \cdot C_a/\{C_a + K^{s}_{1/2}(a) \cdot [1 + C_b/K^{s}_{1/2}(b)]\} \tag{A17}$$

If $C_a + C_b = 165$, Eq. A17 can be rearranged:

$$J^{eff,s}(a) = J^{eff,s}_{max}(a) \cdot [1 - K^{s}_{1/2}(a)/K^{s}_{1/2}(b)]^{-1} \cdot C_a/\{C_a + K^{s}_{1/2}(a) \cdot [1 + 165/K^{s}_{1/2}(b)] \cdot [1 - K^{s}_{1/2}(a)/K^{s}_{1/2}(b)]^{-1}\} \tag{A18a}$$

If transport of anion b is determined, Eq. A18 is modified to:

$$J^{\text{eff,s}}(\text{b}) = J^{\text{eff,s}}_{\max}(\text{b})\cdot[1 - K^{\text{s}}_{1/2}(\text{b})/K^{\text{s}}_{1/2}(\text{a})]^{-1}\cdot C_{\text{b}}/[C_{\text{b}} + K^{\text{s}}_{1/2}(\text{b}) \cdot [1 + 165/K^{\text{s}}_{1/2}(\text{a})]\cdot[1 - K^{\text{s}}_{1/2}(\text{b})/K^{\text{s}}_{1/2}(\text{a})]^{-1}] \quad \text{(A18}b\text{)}$$

Eqs. A18*a* and A18*b* are formally identical to simple Michaelis-Menten equations ($J(\text{a}) = P\text{arm}_1\cdot C_{\text{a}}/(C_{\text{a}} + P\text{arm}_2)$ and $J(\text{b}) = P\text{arm}_3\cdot C_{\text{b}}/(C_{\text{b}} + P\text{arm}_4)$), which contain the two permeability equations, $P(\text{a}) = P\text{arm}_1/(C_{\text{a}} + P\text{arm}_2)$ and $P(\text{b}) = P\text{arm}_3/(C_{\text{b}} + P\text{arm}_4)$. $P\text{arm}_{1\text{–}4}$ represent constants obtained by fitting the permeability equations to the data, presented in Fig. 8 *A*. It follows:

$$P\text{arm}_1 = J^{\text{eff,s}}_{\max}(\text{a})\cdot[1 - K^{\text{s}}_{1/2}(a)/K^{\text{s}}_{1/2}(\text{b})]^{-1} \quad \text{(A19}a\text{)}$$

$$P\text{arm}_2 = K^{\text{s}}_{1/2}(\text{a})\cdot[1 + 165/K^{\text{s}}_{1/2}(\text{b})]\cdot[1 - K^{\text{s}}_{1/2}(\text{a})/K^{\text{s}}_{1/2}(\text{b})]^{-1} \quad \text{(A19}b\text{)}$$

$$P\text{arm}_3 = J^{\text{eff,s}}_{\max}(\text{b})\cdot[1 - K^{\text{s}}_{1/2}(b)/K^{\text{s}}_{1/2}(\text{a})]^{-1} \quad \text{(A19}c\text{)}$$

$$P\text{arm}_4 = K^{\text{s}}_{1/2}(\text{b})\cdot[1 + 165/K^{\text{s}}_{1/2}(\text{a})]\cdot[1 - K^{\text{s}}_{1/2}(\text{b})/K^{\text{s}}_{1/2}(\text{a})]^{-1} \quad \text{(A19}d\text{)}$$

Eqs. A19*b* and A19*d* show that $P\text{arm}_2 + P\text{arm}_4 = -165$, independent of values of $K^{\text{s}}_{1/2}(\text{b})$ and $K^{\text{s}}_{1/2}(\text{a})$. By substitution in Eq. A19*d* one gets Eq. A19*b*, and vice versa. Hence, neither absolute values of $K^{\text{s}}_{1/2}$ nor the ratio between $K^{\text{s}}_{1/2}(\text{b})/K^{\text{s}}_{1/2}(\text{a})$ can be determined in those substitution experiments (unless the ratio is 1 and the permeabilities, therefore, are constant).

Eqs. A19*b* and A19*d* can be rearranged and used to describe (only) the relationship between the two half-saturation constants as shown in Fig. 8 *B*. If chloride transport is studied one has:

$$K^{\text{s}}_{1/2}(\text{b}) = K^{\text{s}}_{1/2}(\text{a})\cdot(165 + P\text{arm}_2)/[P\text{arm}_2 - K^{\text{s}}_{1/2}(\text{a})] \quad \text{(A20}a\text{)}$$

where b refers to bicarbonate and a to chloride. If bicarbonate transport is studied:

$$K^{\text{s}}_{1/2}(\text{b}) = K^{\text{s}}_{1/2}(\text{a})\cdot P\text{arm}_4/[P\text{arm}_4 + K^{\text{s}}_{1/2}(\text{a}) + 165] \quad \text{(A20}b\text{)}$$

Ideally the two curves on Fig. 8 *B* should be identical.

We thank Dr. Michael Hansen for valuable help in evaluation of the mathematical terms of the model, and Dr. Steen Dissing for help in obtaining the fluorescence data. Mrs. Birgitte D. Olsen, Mrs. Lise Mikkelsen, Mrs. Kirsten Heerup, Miss Katja Røhsle Hansen, Miss Gitte Ivarsen, and Miss Henriette Wedel are thanked for their skillful bechnical assistance.

Financial support from NOVO's Fond and Købmand K. Øster-Larsen og hustrus Fond is gratefully acknowledged. P. Gasbjerg was the recipient of grants from The Danish Research Academy and The Natural Sciences Faculty, University of Copenhagen. J. Brahm was a recipient of an Alfred Benzon Senior Investigator Fellowship.

Original version received 7 July 1988 and accepted version received 3 July 1990.

REFERENCES

Brahm, J. 1977. Temperature-dependent changes of chloride transport kinetics in human red cells. *Journal of General Physiology.* 70:283–306.

Brahm, J. 1982. Diffusional water permeability of human erythrocytes and their ghosts. *Journal of General Physiology.* 79:791–819.

Brahm, J. 1986. The physiology of anion transport in red cells. *Progress in Hematology.* 14:1–21.

Brazy, P. C., and R. B. Gunn. 1976. Furosemide inhibition of chloride transport in human red blood cells. *Journal of General Physiology.* 68:583–599.

Britton, H. G. 1964. Permeability of the human red cell to labelled glucose. *Journal of Physiology.* 170:1–20.

Dalmark, M. 1976. Effects of halides and bicarbonate on chloride transport in human red blood cells. *Journal of General Physiology.* 67:223–234.

Dalmark, M., and J. O. Wieth. 1972. Temperature dependence of chloride, bromide, iodide, thiocyanate and salicylate transport in human red cells. *Journal of Physiology.* 224:583–610.

Falke, J. J., K. J. Kanes, and S. I. Chan. 1985. The kinetic equation for the chloride transport cycle of band 3. A ^{35}Cl and ^{37}Cl NMR study. *Journal of Biological Chemistry.* 260:9545–9551.

Fröhlich, O. 1982. The external anion binding site of the human anion transporter: DNDS binding and competition with chloride. *Journal of Membrane Biology.* 65:111–123.

Fröhlich, O. 1984. Relative contributions of the slippage and tunneling mechanisms to anion net efflux from human erythrocytes. *Journal of General Physiology.* 84:877–893.

Fröhlich, O., and R. B. Gunn. 1986. Erythrocyte anion transport: the kinetics of a single-site obligatory exchange system. *Biochimica et Biophysica Acta.* 864:169–194.

Funder, J., and J. O. Wieth. 1966. Chloride and hydrogen ion distribution between human red cells and plasma. *Acta Physiologica Sacndinavica.* 68:234–245.

Funder, J., and J. O. Wieth. 1967. Trapping of sodium, potassium, sucrose, and albumin in the packed cell column of the hematocrit. *Acta Physiologica Scandinavica.* 71:105–112.

Funder, J., and J. O. Wieth. 1976. Chloride transport in human erythrocytes and ghosts: a quantitative comparison. *Journal of Physiology.* 262:679–698.

Furuya, W., T. Tarshis, F.-Y. Law, and P. A. Knauf. 1984. Transmembrane effects of intracellular chloride on the inhibitory potency of extracellular H_2DIDS. Evidence for two conformations of the transport site of the human erythrocyte anion exchange protein. *Journal of General Physiology.* 83:657–681.

Grygorczyk, R., W. Schwarz, and H. Passow. 1987. Potential dependence of the "electrically silent" anion exchange across the plasma membrane of *Xenopus* oocytes mediated by the band-3 protein of mouse red blood cells. *Journal of Membrane Biology.* 99:127–136.

Gunn, R. B., M. Dalmark, D. C. Tosteson, and J. O. Wieth. 1973. Characteristics of chloride transport in human red blood cells. *Journal of General Physiology.* 61:185–206.

Gunn, R. B., and O. Fröhlich. 1979. Asymmetry in the mechanism for anion exchange in human red blood cell membranes. Evidence for reciprocating sites that react with one transported anion at a time. *Journal of General Physiology.* 74:351–374.

Gutknecht, J., M. A. Bisson, and D. C. Tostenson. 1977. Diffusion of carbon dioxide through lipid bilayer membranes. Effects of carbonic anhydrase, bicarbonate and unstirred layers. *Journal of General Physiology.* 69:779–794.

Harned, H. S., and F. T. Bonner. 1945. The first ionization of carbonic acid in aqueous solutions of sodium chloride. *Journal of The American Chemical Society.* 67:1026–1031.

Harned, H. S., and S. R. Scholes, Jr. 1941. The ionization constant of HCO_3^- from 0 to 50°C. *Journal of the American Chemical Society.* 63:1706–1709.

Hautmann, M., and K. F. Schnell. 1985. Concentration dependence of the chloride self exchange and homoexchange fluxes in human red cell ghosts. *Pflügers Archiv.* 405:193–201.

Hunter, M. J. 1977. Human erythrocyte anion permeabilities measured under conditions of net charge transfer. *Journal of Physiology.* 268:35–49.

Janas, T., J. Brahm, P. J. Bjerrum, and J. O. Wieth. 1989. Kinetics of reversible 4,4′-diisothiocyano-2,2′-stilbenedisulfonic acid (DIDS) inhibition of chloride self exchange in human red blood cells. *American Journal of Physiology.* 257:C601–C606.

Jones, G. S., and P. A. Knauf. 1985. Mechanism of the increase in cation permeability of human erythrocytes in low-chloride media. *Journal of General Physiology.* 86:721–738.

Knauf, P. A. 1979. Erythrocyte anion exchange and the band 3 protein: transport kinetics and molecular structure. *Current Topics in Membranes and Transport.* 12:249–363.

Knauf, P. A. 1986. Anion transport in erythrocytes. *In* Physiology of Membrane Disorders. 2nd ed. T. E. Andreoli, J. F. Hoffmann, D. D. Fanestil, and S. G. Schultz, editors. Plenum Publishing Corp., New York. 191–220.

Knauf, P. A., and J. Brahm. 1989. Functional asymmetry of the anion exchange protein, capnophorin: effects on substrate and inhibitor binding. *Methods in Enzymology.* 173:432–453.

Knauf, P. A., G. F. Fuhrmann, S. Rothstein, and A. Rothstein. 1977. The relationship between anion exchange and net anion flow across the human red blood cell membrane. *Journal of General Physiology.* 69:363–386.

Knauf, P. A., F.-Y. Law, T. Tarshis, and W. Furuya. 1984. Effects of the transport site conformation on the binding of external NAP-taurine to the human erythrocyte anion exchange system. Evidence for intrinsic asymmetry. *Journal of General Physiology.* 83:683–701.

Knauf, P. A., and N. Mann. 1986. Location of the chloride self-inhibitory site of the human erythrocyte anion exchange system. *American Journal of Physiology.* 251 (*Cell Physiology* 20): C1–C9.

Macara, I. G., and L. C. Cantley. 1983. The structure and function of band 3. *In* Cell Membranes: Methods and Reviews. E. Elson, W. Frazier, and L. Glaser, editors. Plenum Publishing Corp., New York. 41–87.

Magid, E., and B. O. Turbeck, 1968. The rates of the spontaneous hydration of CO_2 and the reciprocal reaction in neutral aqueous solutions between 0° and 38°. *Biochimica et Biophysica Acta.* 165:515–524.

Passow, H. 1986. Molecular aspects of the band 3 protein-mediated anion transport across the red blood cell membrane. *Reviews of Physiology, Biochemistry and Pharmacology.* 103:61–203.

Schnell, K. F. 1979. The anion transport system of the red blood cell. *In* Proceedings of the Fifth Winter School on Biophysics of Membrane Transport. Agricultural University of Wroclaw, Wroclaw, Poland. Part II:215–252.

Schwoch, G., and H. Passow. 1973. Preparation and properties of human erythrocyte ghosts. *Molecular and Cellular Biochemistry.* 2:197–218.

Wieth, J. O. 1979. Bicarbonate exchange through the human red cell membrane determined with [^{14}C] bicarbonate. *Journal of Physiology.* 294:521–539.

Wieth, J. O. and P. J. Bjerrum. 1983. Transport and modifier sites in capnophorin, the anion transport protein of the erythrocyte membrane. *In* Structure and Function of Membrane Proteins. E. Quagliariello and F. Palmieri, editors. Elsevier Science Publishers B. V., Amsterdam. 95–106.

Wieth, J. O. and J. Brahm. 1980. Kinetics of bicarbonate exchange in human red cells: physiological implications. *In* Membrane Transport in Erythrocytes. Alfred Benzon Symposium 14. U. Lassen, H.H. Ussing, and J.O. Wieth, editors. Munksgaard, Copenhagen. 467–487.

Wieth, J. O., J. Funder, R. B. Gunn, and J. Brahm. 1974. Passive transport pathways for chloride and urea through the red cell membrane. *In* Comparative Biochemistry and Physiology of Transport. L. Bolis, K. Bloch, S. E. Luria, and F. Lynen, editors. North-Holland Publishing Company, Amsterdam. 317–337.